

# Observer-Based Output-Feedback Backstepping Stabilization of Continua of Hyperbolic PDEs and Application to Large-Scale $n + m$ Coupled Hyperbolic PDEs\*

Jukka-Pekka Humaloja<sup>a</sup>, Nikolaos Bekiaris-Liberis<sup>a</sup>

<sup>a</sup>Department of Electrical and Computer Engineering, Technical University of Crete, University Campus, Akrotiri, Chania, 73100, Greece

---

## Abstract

We develop a non-located, observer-based output-feedback law for a class of continua of linear hyperbolic PDE systems, which are viewed as the continuum version of  $n + m$ , general heterodirectional hyperbolic systems as  $n \rightarrow \infty$ . The design relies on the introduction of a novel, continuum PDE backstepping transformation, which enables the construction of a Lyapunov functional for the estimation error system. Stability under the observer-based output-feedback law is established by using the Lyapunov functional construction for the estimation error system and proving well-posedness of the complete closed-loop system, which allows utilization of the separation principle.

Motivated by the fact that the continuum-based designs may provide computationally tractable control laws for large-scale,  $n + m$  systems, we then utilize the control/observer kernels and the observer constructed for the continuum system to introduce an output-feedback control design for the original  $n + m$  system. We establish exponential stability of the resulting closed-loop system, which consists of a mixed  $n + m$ -continuum PDE system (comprising the plant-observer dynamics), introducing a virtual continuum system with resets, which enables utilization of the continuum approximation property of the solutions of the  $n + m$  system by its continuum counterpart (for large  $n$ ). We illustrate the potential computational complexity/flexibility benefits of our approach via a numerical example of stabilization of a large-scale  $n + m$  system, for which we employ the continuum observer-based controller, while the continuum-based stabilizing control/observer kernels can be computed in closed form.

*Keywords:* Backstepping; Continuum system; Hyperbolic PDEs; Output feedback

---

## 1. Introduction

### 1.1. Motivation

Continua of hyperbolic PDE systems can be viewed as continuum versions of certain, large-scale hyperbolic systems, featuring a large number of PDE state components [1, 2]. A specific, theoretically and practically significant case of the latter, is the class of large-scale,  $n + m$ , heterodirectional, linear hyperbolic systems, which may be utilized to describe, for example, the dynamics of blood [3, 4], traffic [5–7], and water [8, 9] flow networks, as well as the dynamics of epidemics transport [10, 11]. For example, PDE-based traffic flow models for multi-lane traffic give rise to  $n + m$  systems with  $(n - m)/2$  lanes in free-flow and  $m$  lanes in congested conditions, respectively [6]. Whereas PDE models of arterial networks describing blood flow from the heart all the way through to a brachial artery (where a measurement can be obtained in a non-invasive manner) consist of interconnected,  $n + m$  hyperbolic systems [4].

In fact, certain control designs developed for stabilization of continua of hyperbolic PDE systems can be utilized for stabilization of the corresponding large-scale system when the number of state components is sufficiently large [1, 2]. This is an important feature as it allows construction of stabilizing control kernels whose computational complexity does not grow with the number of state components [2, 12]. A natural next step is to introduce a dual approach in which one constructs observers and observer kernels for continua of hyperbolic systems, which could, in principle, be utilized as (approximate) observers and observer kernels for the large-scale system counterpart. This key idea provides to the designer the flexibility to construct and compute both observer kernels and observer dynamics, essentially, independently of  $n$ , which has the potential to achieve design of computationally tractable observer-based control laws for large-scale PDE systems. Motivated by this and the fact that neither an observer-based output-feedback design for continua systems of hyperbolic PDEs is available nor it has been applied to control of large-scale  $n + m$  systems, in the present paper we address the problems of observer and output-feedback designs for such a class of continua of hyperbolic systems, as well as their application to large-scale  $n + m$  systems.

---

\*Funded by the European Union (ERC, C-NORA, 101088147). Views and opinions expressed are however those of the authors only and do not necessarily reflect those of the European Union or the European Research Council Executive Agency. Neither the European Union nor the granting authority can be held responsible for them.

## 1.2. Literature

Full-state feedback laws for a class of continua of linear hyperbolic PDEs have been recently developed in [13] and [1]. In particular, [13] first addressed the problem of stabilization of a continuum version of the  $n + 1$  systems considered in [14] as  $n \rightarrow \infty$ , whereas in [1] we developed a feedback control design approach for stabilization of the continuum counterpart (as  $n \rightarrow \infty$ ) of the  $n+m$  hyperbolic systems considered in [15]. The fact that the control design procedure developed for the continuum system in [13] can be employed for stabilization of the large-scale  $n + 1$  (for finite  $n$ ) system, as it may provide stabilizing control kernels that can approximate to arbitrary accuracy the exact (constructed directly for the large-scale  $n + 1$  system) backstepping kernels (for sufficiently large  $n$ ), was established in [2, 2]. There exists no result heretofore addressing the problems of observer and output-feedback designs for such classes of continua of hyperbolic PDE systems.

The backstepping-based output-feedback stabilization problem of  $n + m$  hyperbolic systems has been solved in [15], where the proposed control law involves solving the  $n+m$  control and observer kernel equations, and constructing a Luenberger-type observer for the  $n+m$  system. More recently, control design methods have been developed for other types of  $n + m$  systems in [16–18]. Moreover, state-feedback stabilization of various types of  $n+m$  systems has been considered, e.g., in [19–23]. Such approaches may result in high derivation complexity and computational burden of the respective control laws, as these increase with  $n$  and  $m$  (see, e.g., [17]), due to the requirements of obtaining the solutions to the control/observer kernels, as well as of implementing the observer dynamics. To overcome these potential computational obstacles, methods based on, e.g., neural networks [24–26] and late-lumping implementations [27] have been considered to efficiently approximate a given control design. Our approach can be viewed as an alternative to the above, in that the main goal is to avoid the increase in computational complexity with respect to  $n$ , as well as to provide the user implementation flexibility, via continuum approximation of the backstepping kernels and the observer dynamics, which is a problem heretofore unattempted.

## 1.3. Contributions

In the present paper we develop a backstepping-based observer design methodology for a class of continua systems, which are viewed as the continuum version of  $n + m$ , linear hyperbolic systems as  $n \rightarrow \infty$ . Specifically, we address the dual to the control design problem from [1] in which we consider availability of  $m$  measurements, anti-collocated to the boundary where control is applied. Introducing a suitable target system we derive the continuum kernel equations, which are shown to be well-posed by recasting them in the form of the control kernel equations from [1]. Our choice of the target system enables construction of a Lyapunov functional for the estimation error

system. We then introduce the respective observer-based output-feedback design combining the observer design developed here with the control design developed in [1]. The key in establishing stability of the complete closed-loop system is to show its well-posedness, which in turn allows us to employ the separation principle. The well-posedness proof relies on recasting the complete closed-loop system as an abstract system in output-feedback form and deriving the respective transfer function matrix.

We then utilize as basis the observer and control designs developed for the continuum to introduce an observer-based control design methodology for the large-scale,  $n + m$  system counterpart. The methodology consists of two main ingredients, namely, the construction of a continuum-based observer (that is employed for estimation of the  $n + m$  system's state) and the construction of continuum-based observer kernels. The key element in the methodology lies in the execution of the first step that constitutes the method introduced here different from the respective method in [1], which considers the full-state feedback control design case. In particular, we establish that an observer constructed on the basis of the continuum system can provide accurate estimates of the state of the  $n+m$  system provided that  $n$  is large and that a suitable sampling is applied. Moreover, we study the stability properties of the resulting, unexplored closed-loop system, consisting of both an  $n + m$  and a continuum PDE system, introducing a virtual continuum system with resets at properly chosen time instants. This enables utilization of the continuum approximation property of the solutions of the  $n + m$  system by its continuum counterpart. Specifically, we show that the (augmented by the virtual continuum) closed-loop system can be expressed as consisting of an exponentially stable nominal part that is affected by an additive (state-dependent) perturbation, which does not destroy exponential stability when  $n$  is sufficiently large, as this allows, at each resetting time instant, to reset the state of the augmented system to a state of smaller magnitude. We also present a numerical example with consistent simulation results, in which the continuum-based control/observer kernels can be computed in closed form and the continuum observer is employed, illustrating the potential benefits of our approach in computational complexity/flexibility.

## 1.4. Organization

In Section 2, we present the class of continua of hyperbolic PDEs considered and the proposed observer-based output-feedback law. In Section 3, we employ continuum-based, backstepping control/observer kernels in designing an observer-based control law for  $n + m$  hyperbolic systems. In Section 4, we propose a continuum observer-based control law for  $n + m$  hyperbolic PDEs, where both the observer design and backstepping kernels are based on the continuum approximation. In Section 5, we present a numerical example and consistent simulation results. In Section 6, we provide concluding remarks and discuss potential topics of future research.

### 1.5. Notation

We use the standard notation  $L^2(\Omega; \mathbb{R})$  for real-valued Lebesgue integrable functions on any domain  $\Omega \subset \mathbb{R}^d$  for some  $d \geq 1$ . The notations  $L^\infty(\Omega; \mathbb{R})$ ,  $C(\Omega; \mathbb{R})$ , and  $C^1(\Omega; \mathbb{R})$  denote essentially bounded, continuous, and continuously differentiable functions, respectively, on  $\Omega$ . We denote vectors and matrices by bold symbols, and any  $n, m \in \mathbb{N}$ , we denote by  $E$  the space  $L^2([0, 1]; \mathbb{R}^{n+m})$  equipped with the inner product

$$\langle (\mathbf{u}_1), (\mathbf{u}_2) \rangle_E = \int_0^1 \left( \frac{1}{n} \sum_{i=1}^n u_1^i(x) u_2^i(x) + \sum_{j=1}^m v_1^j(x) v_2^j(x) \right) dx, \quad (1)$$

which induces the norm  $\|\cdot\|_E = \sqrt{\langle \cdot, \cdot \rangle_E}$ . We also define the continuum version of  $E$  as  $n \rightarrow \infty$  by  $E_c = L^2([0, 1]; L^2([0, 1]; \mathbb{R})) \times L^2([0, 1]; \mathbb{R}^m)$ , (i.e.,  $\mathbb{R}^n$  becomes  $L^2([0, 1]; \mathbb{R})$  as  $n \rightarrow \infty$ ) equipped with the inner product

$$\langle (u_1), (u_2) \rangle_{E_c} = \int_0^1 \left( \int_0^1 u_1(x, y) u_2(x, y) dy + \sum_{j=1}^m v_1^j(x) v_2^j(x) \right) dx, \quad (2)$$

which coincides with  $L^2([0, 1]^2; \mathbb{R}) \times L^2([0, 1]; \mathbb{R}^m)$ . Moreover, the transform  $\mathcal{F} = \text{diag}(\mathcal{F}_n, I_m)$  is an isometry from  $E$  to  $E_c$ , where  $\mathcal{F}_n$  maps any  $\mathbf{b} \in \mathbb{R}^n$  to  $L^2([0, 1]; \mathbb{R})$  as

$$\mathcal{F}_n \mathbf{b} = \sum_{i=1}^n b_i \chi_{((i-1)/n, i/n]}, \quad (3)$$

where  $\chi_{((i-1)/n, i/n]}$  denotes the indicator function of the interval  $((i-1)/n, i/n]$ . The adjoint of  $\mathcal{F}$  is of the form  $\mathcal{F}^* = \text{diag}(\mathcal{F}_n^*, I_m)$  with

$$\mathcal{F}_n^* g = \begin{pmatrix} n \int_{(i-1)/n}^{i/n} g(y) dy \\ \vdots \\ n \int_{(i-1)/n}^{i/n} g(y) dy \end{pmatrix}_{i=1}^n, \quad (4)$$

where the  $i$ -th component is the mean value of the function  $g \in L^2([0, 1]; \mathbb{R})$  over the interval  $[(i-1)/n, i/n]$ . Finally, we denote by  $\mathcal{L}(X, Z)$  the space of bounded linear operators from any normed space  $X$  to any normed space  $Z$ , and  $\|\cdot\|_{\mathcal{L}(X, Z)}$  denotes the corresponding operator norm.

We say that a system is exponentially stable on a normed space  $Z$  if, for any initial condition  $z_0 \in Z$ , the (weak) solution  $z \in C([0, \infty); Z)$  of the system satisfies  $\|z(t)\|_Z \leq M e^{-ct} \|z_0\|_E$  for some constants  $M, c > 0$  that are independent of  $z_0$ . Finally, we denote by  $\mathcal{T}$  the triangular set

$$\mathcal{T} = \{(x, \xi) \in [0, 1]^2 : 0 \leq \xi \leq x \leq 1\}. \quad (5)$$

## 2. Observer-Based Output-Feedback Stabilization of Continua Systems of Hyperbolic PDEs

### 2.1. Continua Systems of Hyperbolic PDEs

The considered class of continuum systems is of the form

$$u_t(t, x, y) + \lambda(x, y) u_x(t, x, y) = \int_0^1 \sigma(x, y, \eta) u(t, x, \eta) d\eta + \mathbf{W}(x, y) \mathbf{v}(t, x), \quad (6a)$$

$$\mathbf{v}_t(t, x) - \mathbf{\Lambda}_-(x) \mathbf{v}_x(t, x) = \int_0^1 \mathbf{\Theta}(x, y) u(t, x, y) dy + \mathbf{\Psi}(x) \mathbf{v}(t, x), \quad (6b)$$

with boundary conditions

$$u(t, 0, y) = \mathbf{Q}(y) \mathbf{v}(t, 0), \quad (7a)$$

$$\mathbf{v}(t, 1) = \int_0^1 \mathbf{R}(y) u(t, 1, y) dy + \mathbf{U}(t), \quad (7b)$$

and output  $\mathbf{Y}(t) = \mathbf{v}(t, 0)$ , for almost every  $y \in [0, 1]$ . Here we employ the matrix notation for  $\mathbf{v}$ ,  $\mathbf{U}$ ,  $\mathbf{Y}$ ,  $\mathbf{\Lambda}_-$ ,  $\mathbf{\Theta}$ ,  $\mathbf{\Psi}$ ,  $\mathbf{W}$ ,  $\mathbf{Q}$ , and  $\mathbf{R}$  for the sake of conciseness, that is,  $\mathbf{v} = (v^j)_{j=1}^m$ ,  $\mathbf{U} = (U^j)_{j=1}^m$ ,  $\mathbf{Y} = (Y^j)_{j=1}^m$ , and the parameters are as follows.

**Assumption 1.** *The parameters of (6), (7) are such that*

$$\mathbf{\Lambda}_- = \text{diag}(\mu_j)_{j=1}^m \in C^1([0, 1]; \mathbb{R}^{m \times m}), \quad (8a)$$

$$\mathbf{\Theta} = (\Theta_j)_{j=1}^m \in C([0, 1]; L^2([0, 1]; \mathbb{R}^m)), \quad (8b)$$

$$\mathbf{\Psi} = (\Psi_{i,j})_{i,j=1}^m \in C([0, 1]; \mathbb{R}^{m \times m}), \quad (8c)$$

$$\mathbf{W} = [W_1 \ \cdots \ W_m] \in C([0, 1]; L^2([0, 1]; \mathbb{R}^{1 \times m})), \quad (8d)$$

$$\mathbf{Q} = [Q_1 \ \cdots \ Q_m] \in L^2([0, 1]; \mathbb{R}^{1 \times m}), \quad (8e)$$

$$\mathbf{R} = (R_j)_{j=1}^m \in L^2([0, 1]; \mathbb{R}^m), \quad (8f)$$

with  $\lambda \in C^1([0, 1]^2; \mathbb{R})$  and  $\sigma \in C([0, 1]; L^2([0, 1]^2; \mathbb{R}))$ . Moreover,  $\mu_m(x) > 0$  and  $\lambda(x, y) > 0$  for all  $x, y \in [0, 1]$ , and additionally

$$\min_{x \in [0, 1]} \mu_j(x) > \max_{x \in [0, 1]} \mu_{j+1}(x), \quad (9)$$

for all  $j = 1, \dots, m-1$ . Finally,  $\psi_{j,j} = 0$  for all  $j = 1, \dots, m$ .<sup>1</sup>

<sup>1</sup>This comes without loss of generality, as such terms can be removed using a change of variables (see, e.g., [15, 23]).

## 2.2. Control Law and Observer Design

The control law to stabilize (6), (7) is of the form

$$\begin{aligned} \mathbf{U}(t) = & \int_0^1 \int_0^1 \mathbf{K}(1, \xi, y) \hat{u}(t, \xi, y) dy d\xi \\ & + \int_0^1 \mathbf{L}(1, \xi) \hat{\mathbf{v}}(t, \xi) d\xi - \int_0^1 \mathbf{R}(y) \hat{u}(t, 1, y) dy, \end{aligned} \quad (10)$$

where  $\mathbf{K}, \mathbf{L}$  (satisfying (E.2)–(E.4)) are the backstepping control kernels recalled in Appendix E and  $\hat{u}, \hat{\mathbf{v}}$  is the observer state satisfying the dynamics

$$\begin{aligned} \hat{u}_t(t, x, y) + \lambda(x, y) \hat{u}_x(t, x, y) + \mathbf{P}_+(x, y) (\hat{\mathbf{v}}(t, 0) - \mathbf{v}(t, 0)) = \\ \int_0^1 \sigma(x, y, \eta) \hat{u}(t, x, \eta) d\eta + \mathbf{W}(x, y) \hat{\mathbf{v}}(t, x), \end{aligned} \quad (11a)$$

$$\begin{aligned} \hat{\mathbf{v}}_t(t, x) - \mathbf{A}_-(x) \hat{\mathbf{v}}_x(t, x) + \mathbf{P}_-(x) (\hat{\mathbf{v}}(t, 0) - \mathbf{v}(t, 0)) = \\ \int_0^1 \mathbf{\Theta}(x, y) \hat{u}(t, x, y) dy + \mathbf{\Psi}(x) \hat{\mathbf{v}}(t, x), \end{aligned} \quad (11b)$$

with boundary conditions

$$\hat{u}(t, 0, y) = \mathbf{Q}(y) \mathbf{v}(t, 0), \quad (12a)$$

$$\hat{\mathbf{v}}(t, 1) = \int_0^1 \mathbf{R}(y) \hat{u}(t, 1, y) dy + \mathbf{U}(t), \quad (12b)$$

where  $\mathbf{P}_+, \mathbf{P}_-$  are given by

$$\mathbf{P}_+(x, y) = \mathbf{M}(x, 0, y) \mathbf{A}_-(0), \quad (13a)$$

$$\mathbf{P}_-(x) = \mathbf{N}(x, 0) \mathbf{A}_-(0), \quad (13b)$$

where  $\mathbf{M} \in L^\infty(\mathcal{T}; L^2([0, 1]; \mathbb{R}^{1 \times m}))$ ,  $\mathbf{N} \in L^\infty(\mathcal{T}; \mathbb{R}^{m \times m})$ , is the solution to the observer kernel equations

$$\begin{aligned} \lambda(x, y) \mathbf{M}_x(x, \xi, y) - \mathbf{M}_\xi(x, \xi, y) \mathbf{A}_-(\xi) - \mathbf{M}(x, \xi, y) \mathbf{A}'_-(\xi) = \\ \int_0^1 \sigma(\xi, y, \eta) \mathbf{M}(x, \xi, \eta) d\eta + \mathbf{W}(\xi, y) \mathbf{N}(x, \xi), \end{aligned} \quad (14a)$$

$$\begin{aligned} \mathbf{A}_-(x) \mathbf{N}_x(x, \xi) + \mathbf{N}_\xi(x, \xi) \mathbf{A}_-(\xi) + \mathbf{N}(x, \xi) \mathbf{A}'_-(\xi) = \\ \int_0^1 \mathbf{\Theta}(\xi, y) \mathbf{M}(x, \xi, y) dy + \mathbf{\Psi}(\xi) \mathbf{N}(x, \xi), \end{aligned} \quad (14b)$$

with boundary conditions

$$\mathbf{W}(x, y) = \mathbf{M}(x, x, y) \mathbf{A}_-(x) + \lambda(x, y) \mathbf{M}(x, x, y), \quad (15a)$$

$$\mathbf{\Psi}(x) = \mathbf{N}(x, x) \mathbf{A}_-(x) - \mathbf{A}_-(x) \mathbf{N}(x, x), \quad (15b)$$

$$N_{i,j}(1, \xi) = \int_0^1 R_i(y) M_j(1, \xi, y) dy, \quad \forall i \geq j, \quad (15c)$$

$$N_{i,j}(x, 0) = n_{i,j}(x), \quad \forall i < j, \quad (15d)$$

where  $n_{i,j}(x)$  are arbitrary due to (15d) being an artificial boundary condition to guarantee well-posedness of the observer kernel equations; similarly to the  $n + m$  case in [15]. We choose  $n_{i,j}(x)$  such that

$$n_{i,j}(0) = \frac{\Psi_{i,j}(0)}{\mu_j(0) - \mu_i(0)}, \quad (16)$$

in order to make the artificial boundary condition compatible with (15b) at  $(0, 0)$ . Note that the boundary conditions for  $\mathbf{N}(1, 1)$  are, in general, overdetermined due to (15b) and (15c), (15a), which stems potential discontinuities in the  $\mathbf{N}$  kernels.

## 2.3. Well-Posedness of Observer Kernel Equations

**Theorem 1.** *Under Assumption 1, equations (14)–(16) have a well-posed solution  $\mathbf{M} \in L^\infty(\mathcal{T}; L^2([0, 1]; \mathbb{R}^{1 \times m}))$ ,  $\mathbf{N} \in L^\infty(\mathcal{T}; \mathbb{R}^{m \times m})$ . Moreover, the solution is piecewise continuous in  $(x, \xi) \in \mathcal{T}$ , where the set of discontinuities is of measure zero.*

*Proof.* We first transform the kernel equations (14)–(16) into an analogous form with the control kernel equations, which have been shown to be well-posed in [1, Thm 2]. This transformation is achieved by introducing alternative variables

$$\bar{\mathbf{M}}(\chi, \zeta, y) = \mathbf{M}(1 - \zeta, 1 - \chi, y) = \mathbf{M}(x, \xi, y), \quad (17a)$$

$$\bar{\mathbf{N}}(\chi, \zeta) = \mathbf{N}(1 - \zeta, 1 - \chi) = \mathbf{N}(x, \xi), \quad (17b)$$

and analogously introducing the alternative parameters  $\bar{\mu}, \bar{\lambda}, \bar{\sigma}, \bar{\Theta}, \bar{W}, \bar{\Psi}, \bar{n}_{i,j}$  based on the coordinate transform  $(x, \xi) \rightarrow (1 - \zeta, 1 - \chi)$ , so that  $(\chi, \zeta)$  is the mirror image of  $(x, \xi)$  with respect to the line  $x + \xi = 1$ , and hence,  $(x, \xi) \in \mathcal{T}$  is mirrored into  $(\chi, \zeta) \in \mathcal{T}$ . Inserting these new coordinates into the observer kernel equations (14), (15) and noting  $\partial_x = -\partial_\zeta, \partial_\xi = -\partial_\chi$ , we get the component-wise equations, for  $i, j = 1, \dots, m$ ,

$$\begin{aligned} \bar{\mu}_j(\chi) \partial_\chi \bar{M}_j(\chi, \zeta, y) - \bar{\lambda}(\zeta, y) \partial_\zeta \bar{M}_j(\chi, \zeta, y) + \bar{M}_j(\chi, \zeta, y) \bar{\mu}'_j(\chi) = \\ \int_0^1 \bar{\sigma}(\chi, y, \eta) \bar{M}_j(\chi, \zeta, \eta) d\eta + \sum_{\ell=1}^m \bar{W}_\ell(\chi, y) \bar{N}_{\ell,j}(\chi, \zeta), \end{aligned} \quad (18a)$$

$$\begin{aligned} \bar{\mu}_j(\chi) \partial_\chi \bar{N}_{i,j}(\chi, \zeta) + \bar{\mu}_i(\zeta) \partial_\zeta \bar{N}_{i,j}(\chi, \zeta) + \bar{\mu}'_j(\chi) \bar{N}_{i,j}(\chi, \zeta) = \\ - \int_0^1 \bar{\Theta}_i(\chi, y) \bar{M}_j(\chi, \zeta, y) dy - \sum_{\ell=1}^m \bar{\Psi}_{i,\ell}(\chi) \bar{N}_{\ell,j}(\chi, \zeta), \end{aligned} \quad (18b)$$

with boundary conditions

$$\forall j: \quad \bar{M}_j(\chi, \chi, y) = \frac{\bar{W}_j(\chi, y)}{\bar{\mu}_j(\chi) + \bar{\lambda}(\chi, y)}, \quad (19a)$$

$$\forall i \neq j: \quad \bar{N}_{i,j}(\chi, \chi) = \frac{\bar{\Psi}_{i,j}(\chi)}{\bar{\mu}_j(\chi) - \bar{\mu}_i(\chi)}, \quad (19b)$$

$$\forall i \geq j: \quad \bar{N}_{i,j}(\chi, 0) = \int_0^1 R_i(y) \bar{M}_j(\chi, 0, y) dy, \quad (19c)$$

$$\forall i < j: \quad \bar{N}_{i,j}(1, \zeta) = \bar{n}_{i,j}(\zeta), \quad (19d)$$

where, by (16),  $\bar{n}_{i,j}$  satisfies the compatibility condition

$$\bar{n}_{i,j}(1) = \frac{\bar{\Psi}_{i,j}(1)}{\bar{\mu}_j(1) - \bar{\mu}_i(1)}. \quad (20)$$

The equations (18), (19) are of the same form as the control kernel equations for  $\mathbf{K}, \mathbf{L}$  recalled in Appendix E. In particular, the characteristic curves of (18b) are given by

$$\bar{\rho}_j^p(\chi) = \bar{\phi}_p^{-1}(\bar{\phi}_j(\chi)), \quad (21)$$

for  $1 \leq j \leq p \leq m$ , where

$$\bar{\phi}_j(\chi) = \int_0^\chi \frac{ds}{\bar{\mu}_j(s)}, \quad j = 1, \dots, m. \quad (22)$$

The characteristic curves of (18b) are the potential discontinuity lines of  $\bar{N}_{i,j}$  for  $i > j$ , but we can split the kernels into subdomains of continuity by segmenting the domain  $\mathcal{T}$  of the kernel equations as

$$\bar{\mathcal{T}}_j^p = \left\{ (\chi, \zeta) \in [0, 1]^2 : \bar{\rho}_j^{p+1}(\chi) \leq \zeta \leq \bar{\rho}_j^p(\chi) \right\}, \quad (23)$$

for  $1 \leq j \leq p \leq m$ , where we denote  $\bar{\rho}_j^{m+1} = 0$  for all  $j = 1, \dots, m$ . Now, it follows by [1, Thm 2] that (18), (19) has a well-posed solution  $\bar{\mathbf{M}} \in L^\infty(\mathcal{T}; L^2([0, 1]; \mathbb{R}^{1 \times m}))$ ,  $\bar{\mathbf{N}} \in L^\infty(\mathcal{T}; \mathbb{R}^{m \times m})$ , where  $\bar{\mathbf{M}}, \bar{\mathbf{N}}$  are continuous in  $(\chi, \zeta) \in \bar{\mathcal{T}}_j^p$  for all  $1 \leq j \leq p \leq m$ , and hence, piecewise continuous in  $(\chi, \zeta) \in \mathcal{T}$ . Consequently,  $\bar{\mathbf{M}}, \bar{\mathbf{N}}$  given by (17) is the piecewise continuous solution to (14), (15).  $\square$

#### 2.4. Stability of the Closed-Loop System

**Theorem 2.** *Under Assumption 1, the closed-loop system (6), (7) under the observer-based output-feedback control law (10)–(12) is exponentially stable on  $E_c \times E_c$ .*

The proof is presented at the end of this subsection by utilizing the well-posedness of the closed-loop system given by Proposition 1 in Appendix B, which allows utilization of the separation principle. We first prove the exponential stability of the estimation error dynamics.

**Lemma 1.** *Under Assumption 1, the estimation error dynamics for  $\tilde{u} = \hat{u} - u$  and  $\tilde{\mathbf{v}} = \hat{\mathbf{v}} - \mathbf{v}$  given by*

$$\tilde{u}_t(t, x, y) + \lambda(x, y) \tilde{u}_x(t, x, y) + \mathbf{P}_+(x, y) \tilde{\mathbf{v}}(t, 0) = \int_0^1 \sigma(x, y, \eta) \tilde{u}(t, x, \eta) d\eta + \mathbf{W}(x, y) \tilde{\mathbf{v}}(t, x), \quad (24a)$$

$$\tilde{\mathbf{v}}_t(t, x) - \mathbf{\Lambda}_-(x) \tilde{\mathbf{v}}_x(t, x) + \mathbf{P}_-(x) \tilde{\mathbf{v}}(t, 0) = \int_0^1 \mathbf{\Theta}(x, y) \tilde{u}(t, x, y) dy + \mathbf{\Psi}(x) \tilde{\mathbf{v}}(t, x), \quad (24b)$$

with boundary conditions

$$\tilde{u}(t, 0, y) = 0, \quad (25a)$$

$$\tilde{\mathbf{v}}(t, 1) = \int_0^1 \mathbf{R}(y) \tilde{u}(t, 1, y) dy. \quad (25b)$$

are exponentially stable on  $E_c$ .

*Proof.* We transform (24), (25) into the following target system

$$\tilde{\alpha}_t(t, x, y) + \lambda(x, y) \tilde{\alpha}_x(t, x, y) = \int_0^1 \sigma(x, y, \eta) \tilde{\alpha}(t, x, \eta) d\eta + \int_0^1 \int_0^x D_+(x, \xi, y, \eta) \tilde{\alpha}(t, \xi, \eta) d\xi d\eta, \quad (26a)$$

$$\tilde{\beta}_t(t, x) - \mathbf{\Lambda}_-(x) \tilde{\beta}_x(t, x) = \int_0^1 \mathbf{\Theta}(x, y) \tilde{\alpha}(t, x, y) dy + \int_0^1 \int_0^x \mathbf{D}_-(x, \xi, y) \tilde{\alpha}(t, \xi, y) d\xi dy, \quad (26b)$$

with boundary conditions

$$\tilde{\alpha}(t, 0, y) = 0, \quad (27a)$$

$$\tilde{\beta}(t, 1) = \int_0^1 \mathbf{R}(y) \tilde{\alpha}(t, 1, y) dy - \int_0^1 \mathbf{H}(\xi) \tilde{\beta}(t, \xi) d\xi, \quad (27b)$$

where  $D_+ \in L^\infty(\mathcal{T}; L^2([0, 1]^2; \mathbb{R}))$ ,  $\mathbf{D}_- \in L^\infty(\mathcal{T}; L^2([0, 1]; \mathbb{R}^m))$  are given by

$$\mathbf{D}_-(x, \xi, y) = -\mathbf{N}(x, \xi) \mathbf{\Theta}(\xi, y) - \int_\xi^x \mathbf{N}(x, s) \mathbf{D}_-(s, \xi, y) ds, \quad (28a)$$

$$D_+(x, \xi, y, \eta) = -\mathbf{M}(x, \xi, y) \mathbf{\Theta}(\xi, \eta) - \int_\xi^x \mathbf{M}(x, s, y) \mathbf{D}_-(s, \xi, \eta) ds, \quad (28b)$$

and  $\mathbf{H} \in L^\infty([0, 1]; \mathbb{R}^{m \times m})$  is strictly upper triangular, i.e.,  $H_{i,j} = 0$  for all  $i \geq j$ , with its values for  $i < j$  to be determined. The transformation is given by

$$\tilde{u}(t, x, y) = \tilde{\alpha}(t, x, y) + \int_0^x \mathbf{M}(x, \xi, y) \tilde{\beta}(t, \xi) d\xi, \quad (29a)$$

$$\tilde{\mathbf{v}}(t, x) = \tilde{\beta}(t, x) + \int_0^x \mathbf{N}(x, \xi) \tilde{\beta}(t, \xi) d\xi, \quad (29b)$$

where  $\mathbf{M}, \mathbf{N}$  are the observer kernels. In order for (29) to transform (24), (25) into (26), (27), the observer kernels need to satisfy (14), (15) as shown in Appendix A, where we also obtain (13) and (28) for  $D_+, \mathbf{D}_-$ . Note that as  $\mathbf{M} \in L^\infty(\mathcal{T}; L^2([0, 1]; \mathbb{R}^{1 \times m}))$ ,  $\mathbf{N} \in L^\infty(\mathcal{T}; \mathbb{R}^{m \times m})$  are well-posed by Theorem 1, (28a) is a Volterra equation of second kind for  $\mathbf{D}_-$  and it has a well-posed solution  $\mathbf{D}_- \in L^\infty(\mathcal{T}; L^2([0, 1]; \mathbb{R}^m))$  by [1, Lem. 7]. Thereafter  $D_+ \in L^\infty(\mathcal{T}; L^2([0, 1]^2; \mathbb{R}))$  is uniquely determined by (28b) based on  $\mathbf{C}_-, \mathbf{M}$ , and  $\Theta$ . Finally, evaluating (29) along  $x = 1$  and using the boundary conditions (25), (27) gives

$$\mathbf{H}(\xi) = \mathbf{N}(1, \xi) - \int_0^1 \mathbf{R}(y) \mathbf{M}(1, \xi, y) dy, \quad (30)$$

which splits into (15c) and

$$H_{i,j}(\xi) = N_{i,j}(1, \xi) - \int_0^1 R_i(y) M_j(1, \xi, y) dy, \quad \forall i < j, \quad (31)$$

determining the nonzero entries of  $\mathbf{H}$ .

We then establish that the transform (29) is boundedly invertible, which follows as (29b) is a Volterra equation of second kind for  $\tilde{\beta}(\cdot, x)$  in terms of  $\tilde{\mathbf{v}}(\cdot, x)$  and  $\mathbf{N}$ . Thus, by [28, Thm 2.3.6], (29b) has a unique solution  $\tilde{\beta}(t, \cdot) \in L^2([0, 1]; \mathbb{R}^m)$  for all  $t \geq 0$ . Thereafter,  $\tilde{\alpha}(\cdot, t) \in L^2([0, 1]; L^2([0, 1]; \mathbb{R}))$  is uniquely determined by (29a) for all  $t \geq 0$ . Thus, the transform (29) is boundedly invertible, and hence, the exponential stability of (24), (25) is equivalent to the exponential stability of (26), (27).

In order to show that (26), (27) is exponentially stable, consider a Lyapunov functional with parameters  $\delta, \mathbf{B} = \text{diag}(B_1, \dots, B_m) > 0$  of the form

$$V(t) = \int_0^1 \int_0^1 e^{-\delta x} \frac{\tilde{\alpha}^2(t, x, y)}{\lambda(x, y)} dy dx + \int_0^1 e^{\delta x} \tilde{\beta}^T(t, x) \mathbf{B} \mathbf{A}^{-1}(x) \tilde{\beta}(t, x) dx. \quad (32)$$

Computing  $\dot{V}(t)$  and integrating by parts in  $x$  gives

$$\dot{V}(t) = \left[ -e^{-\delta x} \|\tilde{\alpha}(t, x, \cdot)\|_{L^2}^2 + e^{\delta x} \|\tilde{\beta}(t, x)\|_{\mathbf{B}}^2 \right]_0^1$$

$$\begin{aligned} & - \delta \int_0^1 \left( e^{-\delta x} \|\tilde{\alpha}(t, x, \cdot)\|_{L^2}^2 + e^{\delta x} \|\tilde{\beta}(t, x)\|_{\mathbf{B}}^2 \right) dx \\ & + 2 \int_0^1 \int_0^1 \int_0^1 e^{-\delta x} \frac{\tilde{\alpha}(t, x, y)}{\lambda(x, y)} \sigma(x, \eta, y) \tilde{\alpha}(t, x, \eta) d\eta dy dx \\ & + 2 \int_0^1 \int_0^1 \int_0^1 \int_0^x e^{-\delta x} \frac{\tilde{\alpha}(t, x, y)}{\lambda(x, y)} D_+(x, \xi, y, \eta) \tilde{\alpha}(t, \xi, \eta) d\xi d\eta dy dx \\ & + \int_0^1 \int_0^1 e^{\delta x} \left( \tilde{\beta}^T(t, x) \mathbf{B} \mathbf{A}^{-1}(x) \Theta(x, y) \right. \\ & \quad \left. + \Theta^T(x, y) \mathbf{B} \mathbf{A}^{-1}(x) \tilde{\beta}(t, x) \right) \tilde{\alpha}(t, x, y) dy dx \\ & + \int_0^1 \int_0^1 \int_0^x e^{\delta x} \left( \tilde{\beta}^T(t, x) \mathbf{B} \mathbf{A}^{-1}(x) \mathbf{D}_-(x, \xi, y) \right. \\ & \quad \left. + \mathbf{D}_-^T(x, \xi, y) \mathbf{B} \mathbf{A}^{-1}(x) \tilde{\beta}(t, x) \right) \tilde{\alpha}(t, \xi, y) d\xi dy dx, \end{aligned} \quad (33)$$

where  $\|\cdot\|_{\mathbf{B}}^2 = \langle \cdot, \mathbf{B} \cdot \rangle_{\mathbb{R}^m}$  denotes the  $\mathbf{B}$ -weighted inner product. Using the following bounds (that exist by Assumption 1 and Theorem 1)

$$m_\lambda = \min_{x, y \in [0, 1]} \lambda(x, y), \quad (34a)$$

$$m_\mu = \min_{j \in \{1, \dots, m\}} \min_{x \in [0, 1]} \mu_j(x), \quad (34b)$$

$$M_\sigma = \max_{x \in [0, 1]} \left\| \int_0^1 \sigma(x, \cdot, \eta) d\eta \right\|_{L^2}, \quad (34c)$$

$$M_\Theta = \max_{j=1, \dots, m} \max_{x \in [0, 1]} \|\Theta_j(x, \cdot)\|_{L^2}, \quad (34d)$$

$$M_{D_+} = \text{ess sup}_{(x, \xi) \in \mathcal{T}} \left\| \int_0^1 D_+(x, \xi, \cdot, \eta) d\eta \right\|_{L^2}, \quad (34e)$$

$$M_{D_-} = \max_{j \in \{1, \dots, m\}} \text{ess sup}_{(x, \xi) \in \mathcal{T}} \|D_j^-(x, \xi, \cdot)\|_{L^2}, \quad (34f)$$

$$M_H = \max_{i, j \in \{1, \dots, m\}} \text{ess sup}_{x \in [0, 1]} |H_{ij}(x)|, \quad (34g)$$

$$M_R = \max_{j=1, \dots, m} \|R_j\|_{L^2}, \quad (34h)$$

$$M_B = \max_{j=1, \dots, m} B_j, \quad (34i)$$

the boundary conditions (27), the Cauchy-Schwartz inequality, and  $2 \langle f, g \rangle_{L^2} \leq \|f\|_{L^2}^2 + \|g\|_{L^2}^2$  for any  $f, g \in L^2$ , we can estimate (33) as

$$\begin{aligned} \dot{V}(t) & \leq - (e^{-\delta} - 2e^\delta m M_R^2 M_B) \|\tilde{\alpha}(t, 1, \cdot)\|_{L^2}^2 \\ & \quad + 2e^\delta \int_0^1 \|\mathbf{H}(x) \tilde{\beta}(t, x)\|_{\mathbf{B}}^2 dx \\ & \quad - \delta \int_0^1 \left( e^{-\delta x} \|\tilde{\alpha}(t, x, \cdot)\|_{L^2}^2 + e^{\delta x} \|\tilde{\beta}(t, x)\|_{\mathbf{B}}^2 \right) dx \end{aligned}$$

$$\begin{aligned}
& + 2 \int_0^1 e^{-\delta x} \frac{M_\sigma + M_{D+}}{m_\lambda} \|\tilde{\alpha}(t, x, \cdot)\|_{L^2}^2 dx \\
& + \int_0^1 m e^{\delta x} M_B \frac{M_\Theta^2 + M_{D-}^2}{m_\mu^2} \|\tilde{\alpha}(t, x, \cdot)\|_{L^2}^2 dx \\
& + 2 \int_0^1 e^{\delta x} \|\tilde{\beta}(t, x)\|_{\mathbf{B}}^2 dx. \tag{35}
\end{aligned}$$

Due to the triangular structure of  $\mathbf{H}$  we can estimate

$$\|\mathbf{H}(x)\tilde{\beta}(t, x)\|_{\mathbf{B}}^2 \leq M_H^2 \sum_{j=2}^m \sum_{\ell=1}^{j-1} (m-\ell) B_\ell \tilde{\beta}_j^2(t, x), \tag{36}$$

so that we can enforce

$$2e^\delta \|\mathbf{H}(x)\tilde{\beta}(t, x)\|_{\mathbf{B}}^2 \leq \|\tilde{\beta}(t, x)\|_{\mathbf{B}}^2, \tag{37}$$

by assigning

$$B_j = 2e^\delta M_H^2 \sum_{\ell=1}^{j-1} (m-\ell) B_\ell, \quad j = 2, \dots, m. \tag{38}$$

In order to determine  $B_1$ , the first term of (35) needs to be non-positive, which gives

$$M_B \leq \frac{e^{-2\delta}}{2mM_R^2}, \tag{39}$$

where  $M_B = B_m$  by (38), and hence,  $B_1$  can be assigned as

$$B_1 = \frac{e^{-2\delta}}{2mM_R^2 \sum_{\ell=j}^m (2e^\delta M_H^2)^{\ell-1} \frac{(m-1)!}{(m-\ell)!}}. \tag{40}$$

Finally,  $\dot{V}(t)$  can be made negative definite by choosing  $\delta$  such that

$$\delta > \max \left\{ 2 \frac{M_\sigma + M_{D+}}{m_\lambda} + \frac{M_\Theta^2 + M_{D-}^2}{2M_R^2 m_\mu^2}, 3 \right\}, \tag{41}$$

and thus, the dynamics (26), (27) are exponentially stable.  $\square$

*Proof of Theorem 2.* Since the closed-loop system (6), (7), (10)–(12), is well-posed by Proposition 1, we can introduce a change of variables  $\tilde{z} = \hat{z} - z$  and write the closed-loop system equivalently, utilizing the notation of Appendix B, as

$$\begin{bmatrix} \dot{z}(t) \\ \dot{\tilde{z}}(t) \end{bmatrix} = \begin{bmatrix} A_{-1} + B_Q C + BK & -BC_R + BK \\ 0 & A_{-1} + BC_R + PC \end{bmatrix} \begin{bmatrix} z(t) \\ \tilde{z}(t) \end{bmatrix}, \tag{42}$$

where  $\dot{z}(t) = (A_{-1}z(t) + B_Q C + BK)z(t)$  corresponds to the closed-loop dynamics of (6), (7) under the backstepping state feedback law  $\mathbf{U}(t) = \mathcal{K}z(t) - C_R z(t)$  and  $\dot{\tilde{z}}(t) = (A_{-1} + BC_R + PC)\tilde{z}(t)$  corresponds to the estimation error dynamics (24), (25). As these dynamics are exponentially stable by [1, Thm 1] and Lemma 1, respectively, the exponential stability of the closed-loop system follows, e.g., by the Gearhart—Prüss—Greiner Theorem [29, Thm V.1.11], and the decay rate is determined by the smaller one of the diagonal dynamics.

### 3. Output-Feedback Stabilization of Large-Scale $n+m$ Systems Based on Continuum Kernels

#### 3.1. Large-Scale $n+m$ Systems of Hyperbolic PDEs

Consider a system of  $n+m$  hyperbolic PDEs<sup>2</sup>

$$\mathbf{u}_t(t, x) + \mathbf{\Lambda}_+(x)\mathbf{u}_x(t, x) = \frac{1}{n}\mathbf{\Sigma}(x)\mathbf{u}(t, x) + \mathbf{W}(x)\mathbf{v}(t, x), \tag{43a}$$

$$\mathbf{v}_t(t, x) - \mathbf{\Lambda}_-(x)\mathbf{v}_x(t, x) = \frac{1}{n}\mathbf{\Theta}(x)\mathbf{u}(t, x) + \mathbf{\Psi}(x)\mathbf{v}(t, x), \tag{43b}$$

with boundary conditions

$$\mathbf{u}(t, 0) = \mathbf{Q}\mathbf{v}(t, 0), \quad \mathbf{v}(t, 1) = \frac{1}{n}\mathbf{R}\mathbf{u}(t, 1) + \mathbf{U}(t), \tag{44}$$

where we employ the matrix notation for  $\mathbf{u}$ ,  $\mathbf{v}$ ,  $\mathbf{U}$ ,  $\mathbf{\Lambda}_+$ ,  $\mathbf{\Lambda}_-$ ,  $\mathbf{\Sigma}$ ,  $\mathbf{W}$ ,  $\mathbf{\Theta}$ ,  $\mathbf{\Psi}$ ,  $\mathbf{Q}$ , and  $\mathbf{R}$  for the sake of conciseness, that is,  $\mathbf{u} = (u^i)_{i=1}^n$ ,  $\mathbf{v} = (v^j)_{j=1}^m$ ,  $\mathbf{U} = (U^j)_{j=1}^m$ , and the parameters are as follows.

**Assumption 2.** *The parameters of (43), (44) are such that*

$$\mathbf{\Lambda}_+ = \text{diag}(\lambda_i)_{i=1}^n \in C^1([0, 1]; \mathbb{R}^{n \times n}), \tag{45a}$$

$$\mathbf{\Lambda}_- = \text{diag}(\mu_j)_{j=1}^m \in C^1([0, 1]; \mathbb{R}^{m \times m}), \tag{45b}$$

$$\mathbf{\Sigma} = (\sigma_{i,j})_{i,j=1}^n \in C([0, 1]; \mathbb{R}^{n \times n}), \tag{45c}$$

$$\mathbf{W} = (w_{i,j})_{i=1,j=1}^{n,m} \in C([0, 1]; \mathbb{R}^{n \times m}), \tag{45d}$$

$$\mathbf{\Theta} = (\theta_{j,i})_{j=1,i=1}^{m,n} \in C([0, 1]; \mathbb{R}^{m \times n}), \tag{45e}$$

$$\mathbf{\Psi} = (\psi_{i,j})_{i,j=1}^{m,m} \in C([0, 1]; \mathbb{R}^{m \times m}), \tag{45f}$$

$$\mathbf{Q} = (q_{i,j})_{i=1,j=1}^{n,m} \in \mathbb{R}^{n \times m}, \tag{45g}$$

$$\mathbf{R} = (r_{j,i})_{j=1,i=1}^{m,n} \in \mathbb{R}^{m \times n}, \tag{45h}$$

where  $\lambda_i(x), \mu_j(x) > 0$  for all  $x \in [0, 1]$  and  $i = 1, \dots, n, j = 1, \dots, m$ . Moreover,  $\mu_j$  satisfy (9) and  $\psi_{j,j} = 0$ , for  $j = 1, \dots, m$ .

*Remark 1.* Under Assumption 2, it can be shown by using the same arguments as in [2, Prop. A.1] that the system (43), (44) is well-posed on the Hilbert space  $E$ .

#### 3.2. Observer-Based Output-Feedback Controller Based on Continuum Kernels

The observer-based backstepping output-feedback law to stabilize (43), (44) based on continuum kernels is of the form

$$\begin{aligned}
\mathbf{U}(t) &= \frac{1}{n} \int_0^1 \tilde{\mathbf{K}}(1, \xi) \hat{\mathbf{u}}(t, \xi) d\xi + \int_0^1 \tilde{\mathbf{L}}(1, \xi) \hat{\mathbf{v}}(t, \xi) d\xi \\
&\quad - \frac{1}{n} \mathbf{R} \hat{\mathbf{u}}(t, 1), \tag{46}
\end{aligned}$$

<sup>2</sup>We scale the sums involving the  $n$ -part states  $u^i, i = 1, \dots, n$  by  $1/n$  in order to make the considerations in the limit  $n \rightarrow \infty$  more natural, as discussed in [2, Rem. 2.2].

where the control gains  $\tilde{\mathbf{K}}, \tilde{\mathbf{L}}$  are given in (E.7) and the observer dynamics for  $\hat{\mathbf{u}}, \hat{\mathbf{v}}$  are

$$\hat{\mathbf{u}}_t(t, x) + \mathbf{A}_+(x)\hat{\mathbf{u}}_x(t, x) + \tilde{\mathbf{P}}_+(x)(\hat{\mathbf{v}}(t, 0) - \mathbf{v}(t, 0)) = \frac{1}{n}\mathbf{\Sigma}(x)\hat{\mathbf{u}}(t, x) + \mathbf{W}(x)\hat{\mathbf{v}}(t, x), \quad (47a)$$

$$\hat{\mathbf{v}}_t(t, x) - \mathbf{A}_-(x)\hat{\mathbf{v}}_x(t, x) + \tilde{\mathbf{P}}_-(x)(\hat{\mathbf{v}}(t, 0) - \mathbf{v}(t, 0)) = \frac{1}{n}\mathbf{\Theta}(x)\hat{\mathbf{u}} + \mathbf{\Psi}(x)\hat{\mathbf{v}}(t, x), \quad (47b)$$

with boundary conditions

$$\hat{\mathbf{u}}(t, 0) = \mathbf{Q}\mathbf{v}(t, 0), \quad \hat{\mathbf{v}}(t, 1) = \frac{1}{n}\mathbf{R}\hat{\mathbf{u}}(t, 1) + \mathbf{U}(t), \quad (48)$$

where the output injection gains  $\tilde{\mathbf{P}}_+, \tilde{\mathbf{P}}_-$  are taken based on the continuum observer kernels  $\mathbf{M}, \mathbf{N}$ , satisfying (14)–(16), as

$$\tilde{\mathbf{P}}_+(x) = \mathcal{F}_n^* \mathbf{M}(x, 0, \cdot) \mathbf{A}_-(0), \quad (49a)$$

$$\tilde{\mathbf{P}}_-(x) = \mathbf{N}(x, 0) \mathbf{A}_-(0). \quad (49b)$$

We have the following result.

**Theorem 3.** *Consider an  $n + m$  system (43), (44) with parameters satisfying Assumption 2. Construct respective continuum parameters satisfying Assumption 1 and (E.5), and solve the continuum control and observer kernel equations (E.2)–(E.4) and (14)–(16) for  $\mathbf{K}, \mathbf{L}$  and  $\mathbf{M}, \mathbf{N}$ , respectively, under these parameters. When  $n$  is sufficiently large, the observer-based output-feedback law (46)–(49) exponentially stabilizes the  $n + m$  system (43), (44) on  $E$ .*

### 3.3. Proof of Theorem 3

Firstly, we state the following auxiliary result for the estimation error dynamics.

**Lemma 2.** *When  $n$  is sufficiently large, the estimation error dynamics for the observer (47)–(49) are exponentially stable on  $E$ .*

*Proof.* Analogously to the notation of Appendix B, denote  $\mathbf{z}(t) = (\mathbf{u}(t, \cdot), \mathbf{v}(t, \cdot))$  and define

$$\mathbf{A}\mathbf{z}(t) = \begin{bmatrix} -\mathbf{A}_+ \partial_x & 0 \\ 0 & \mathbf{A}_- \partial_x \end{bmatrix} \mathbf{z}(t) + S\mathbf{z}(t), \quad (50)$$

where  $S\mathbf{z}(t)$  corresponds to the right-hand side of (43) and the domain of  $\mathbf{A}$  is defined as  $\mathcal{D}(\mathbf{A}) = \{\mathbf{z} \in H^1([0, 1]; \mathbb{R}^{n+m}) : \mathbf{u}(0) = 0, \mathbf{v}(1) = 0\}$ , and denote by  $\mathbf{A}_{-1}$  the unique extension of  $\mathbf{A}$  to  $E$ . Moreover, define output operators  $\mathbf{C}\mathbf{z}(t) = \mathbf{v}(0, t)$ ,  $\mathbf{C}_R\mathbf{z}(t) = \frac{1}{n}\mathbf{R}\mathbf{u}(t, 1)$ , and additionally  $\mathbf{B} = \begin{bmatrix} 0 \\ \delta_1 \mathbf{A}_- \end{bmatrix}$ ,  $\mathbf{B}_Q = \begin{bmatrix} \delta_0 \mathbf{A}_+ \mathbf{Q} \\ 0 \end{bmatrix}$ , and  $\tilde{\mathbf{P}} = \mathcal{F}^* P$ , where  $\mathcal{F}^* = \text{diag}(\mathcal{F}_n^*, I_m)$  with  $\mathcal{F}_n^*$  defined in (4) and  $P$  is defined in (B.5). The estimation error dynamics for  $\tilde{\mathbf{z}} = \hat{\mathbf{z}} - \mathbf{z}$  can then be written as

$$\begin{aligned} \dot{\tilde{\mathbf{z}}}(t) &= (\mathbf{A}_{-1} + \mathbf{B}\mathbf{C}_R + \tilde{\mathbf{P}}\mathbf{C})\tilde{\mathbf{z}}(t) \\ &= (\mathbf{A}_{-1} + \mathbf{B}\mathbf{C}_R + \mathbf{P}\mathbf{C})\tilde{\mathbf{z}}(t) + \Delta\mathbf{P}\mathbf{C}\tilde{\mathbf{z}}(t), \end{aligned} \quad (51)$$

where we denote  $\Delta\mathbf{P} = \mathbf{P} - \tilde{\mathbf{P}}$ , where  $\mathbf{P}$  denotes the output injection operator corresponding to the exact  $n + m$  observer kernels given in [15, (60)–(70)]. The dynamics (51) are well-posed as  $\mathbf{P}, \tilde{\mathbf{P}}$  are bounded linear operators and  $\mathbf{C}$  is an admissible output operator for  $\mathbf{A}_P := \mathbf{A}_{-1} + \mathbf{B}\mathbf{C}_R + \mathbf{P}\mathbf{C}$  by [30, Thm 5.4.2]. By duality [30, Thm 4.4.3], we have that  $\mathbf{C}^*$  is an admissible control operator for  $\mathbf{A}_P^*$ .<sup>3</sup> Hence, when  $\|\Delta\mathbf{P}\|_{\mathcal{L}(\mathbb{R}^m; E)}$  is sufficiently small, we obtain the exponential stability of  $(\mathbf{A}_P + \Delta\mathbf{P}\mathbf{C})^* = \mathbf{A}_P^* + \mathbf{C}^*\Delta\mathbf{P}^*$  by [2, Prop. A.2].

To conclude the proof, we show that  $\|\Delta\mathbf{P}\|_{\mathcal{L}(\mathbb{R}^m; E)}$  becomes arbitrarily small when  $n$  is sufficiently large. By applying (17), we can transform the observer kernel equations (14), (15) for  $\mathbf{M}, \mathbf{N}$  into alternative kernel equations (18), (19) and compare them with the respectively transformed  $n + m$  observer kernel equations given in [15, (73), (74)]. As the transformed observer kernel equations are of the same form as the respective control kernel equations, we have by [1, Lem. 5] that  $\mathcal{F}_n^* \mathbf{M}(x, 0, \cdot), \mathbf{N}(x, 0)$ , for almost all  $x \in [0, 1]$ , tend arbitrarily close to the exact  $n + m$  observer kernels evaluated along  $\xi = 0$ , when  $n$  is sufficiently large. Consequently, as  $\mathbf{A}_-(0)$  is unaffected by the continuum approximation,  $\|\Delta\mathbf{P}\|_{\mathcal{L}(\mathbb{R}^m; E)}$  becomes arbitrarily small when  $n$  is sufficiently large.  $\square$

*Proof of Theorem 3.* The remaining steps are analogous to the proof of Theorem 2. That is, the well-posedness of the closed-loop system follows by the same steps as in Appendix B after replacing  $E_c$  with  $E$  and the operators with the ones introduced in the proof of Lemma 2. The resulting (open-loop) transfer function is in fact identical to (B.9), so that the same well-posedness arguments for the closed-loop system apply as at the end of Appendix B. Hence, as the closed-loop system is well-posed, we can introduce  $\tilde{\mathbf{z}} = \hat{\mathbf{z}} - \mathbf{z}$  and write the closed-loop system equivalently as

$$\begin{bmatrix} \dot{\mathbf{z}}(t) \\ \dot{\tilde{\mathbf{z}}}(t) \end{bmatrix} = \begin{bmatrix} \mathbf{A}_{-1} + \mathbf{B}_Q\mathbf{C} + \mathbf{B}\tilde{\mathbf{K}} & -\mathbf{B}\mathbf{C}_R + \mathbf{B}\tilde{\mathbf{K}} \\ 0 & \mathbf{A}_{-1} + \mathbf{B}\mathbf{C}_R + \tilde{\mathbf{P}}\mathbf{C} \end{bmatrix} \begin{bmatrix} \mathbf{z}(t) \\ \tilde{\mathbf{z}}(t) \end{bmatrix}, \quad (52)$$

where the diagonal entries are exponentially stable by [1, Thm 3] and Lemma 2, respectively, when  $n$  is sufficiently large. Consequently, due to the triangular structure, the closed-loop system is exponentially stable when  $n$  is sufficiently large.

## 4. Output-Feedback Stabilization of Large-Scale $n + m$ Systems Using Continuum Observer

In this section, we consider continuum observer-based stabilization of large-scale  $n + m$  systems. That is, the ob-

<sup>3</sup>Note that  $\mathbf{A}_P^*$  is the (unbounded) adjoint of  $\mathbf{A}_P$ , i.e., they satisfy  $\langle \mathbf{A}_P \mathbf{z}_1, \mathbf{z}_2 \rangle_E = \langle \mathbf{z}_1, \mathbf{A}_P^* \mathbf{z}_2 \rangle_E$  with  $\mathbf{z}_1 \in \mathcal{D}(\mathbf{A}_P), \mathbf{z}_2 \in \mathcal{D}(\mathbf{A}_P^*)$ ; whereas  $\mathbf{C}^*$  is defined through the dual pairing  $\langle \mathbf{C}\mathbf{z}_1, \mathbf{U} \rangle_{\mathbb{R}^m} = \langle \mathbf{z}_1, \mathbf{C}^* \mathbf{U} \rangle_{\mathcal{D}(\mathbf{A}_P), \mathcal{D}(\mathbf{A}_P)^d}$  with  $\mathbf{z}_1 \in \mathcal{D}(\mathbf{A}_P)$ , where  $\mathcal{D}(\mathbf{A}_P)^d$  denotes the dual space of  $\mathcal{D}(\mathbf{A}_P)$  with respect to the pivot space  $E$  (see, e.g., [30, Sect. 2.9–10]).



server is taken as the continuum observer (11), (12), except that the measurement  $\mathbf{v}(0, t)$  is taken from the  $n + m$  system (43), (44). Moreover, the control law is taken as (10) based on the continuum observer (and kernels). The motivation is that the computation/implementation of continuum observer-based control law is then independent of  $n$ , and thus, so is the respective computational complexity. This implies that we may potentially gain in computational complexity when computing the control law, as opposed to using an  $n + m$  observer, when  $n$  is large, as computational complexity of the  $n + m$  observer grows with  $n$ . In particular, the continuum observer-based control law does not require reconstruction of the  $n + m$  system state. However, the continuum observer can provide an (approximate) estimate for the  $n + m$  system state by sampling the continuum observer state appropriately in  $y$ , e.g., by applying  $\mathcal{F}^*$  to the continuum observer state.<sup>4</sup>

We state next the main result of the section, which is exponential stability of the closed-loop system under the continuum observer-based control law. The proof of this result essentially relies on the fact that the continuum, observer-based output-feedback controller stabilizes a virtual continuum system, together with the fact that the solutions of the closed-loop, virtual continuum system approximate to arbitrary accuracy the closed-loop solutions of the  $n + m$  system (under the same control input), for sufficiently large  $n$ , when the parameters of the  $n + m$  and continuum systems are connected via (E.5) (and thus, for large  $n$ , the parameters of the  $n + m$  system can be approximated by the parameters of the continuum).

**Theorem 4.** *Consider the continuum observer-based control law (10)–(13), where the measurement  $\mathbf{v}(0, t)$  is taken from the  $n + m$  system (43), (44) and the parameters of (10)–(13) are connected to the parameters of (43), (44) via (E.5). When  $n$  is sufficiently large, the closed-loop system comprising (43), (44) and (10)–(13) is exponentially stable on  $E \times E_c$ .*

*Proof.* Step 1 (well-posedness and alternative representation of the closed-loop system): We begin by establishing the well-posedness of the considered closed-loop system. Using the notation introduced in the proof of Lemma 2 and Appendix B, the closed-loop system can be written as

$$\begin{bmatrix} \dot{\mathbf{z}}(t) \\ \dot{\hat{\mathbf{z}}}(t) \end{bmatrix} = \begin{bmatrix} \mathbf{A}_{-1} + \mathbf{B}\mathbf{C}_R + \mathbf{B}_Q\mathbf{C} & \mathbf{B}\mathcal{K} - \mathbf{B}\mathbf{C}_R \\ \mathbf{P}\mathbf{C} + \mathbf{B}_Q\mathbf{C} & A_{-1} - \mathbf{P}\mathbf{C} + \mathbf{B}\mathcal{K} \end{bmatrix} \begin{bmatrix} \mathbf{z}(t) \\ \hat{\mathbf{z}}(t) \end{bmatrix}. \quad (54)$$

The well-posedness of the closed-loop system (54) is established in Appendix C. For the convenience of the subsequent analysis, we transform the  $n + m$  system state to

<sup>4</sup>This results in an additional (mean value) approximation error that also becomes arbitrarily small when  $n$  is sufficiently large (see, e.g., [2, (C.44), (C.45)]):

$$\|\mathbf{z}(t) - \mathcal{F}^*\hat{\mathbf{z}}(t)\|_E \leq \|\mathcal{F}\mathbf{z}(t) - \hat{\mathbf{z}}(t)\|_{E_c} + \|\hat{\mathbf{z}}(t) - \mathcal{F}\mathcal{F}^*\hat{\mathbf{z}}(t)\|_{E_c}. \quad (53)$$

The estimation error in (53) decays exponentially to zero as it is evident within the proof of Theorem 4 (see (76)).

$E_c$  by applying  $\mathcal{F}$  to the dynamics from the left and using  $\mathcal{F}^*\mathcal{F} = I$ . Hence, we define the notations<sup>5</sup>

$$z^n = \mathcal{F}\mathbf{z}, \quad A^n = \mathcal{F}\mathbf{A}\mathcal{F}^*, \quad (55a)$$

$$B^n = \mathcal{F}\mathbf{B} = B, \quad B_Q^n = \mathcal{F}\mathbf{B}_Q, \quad (55b)$$

$$\mathcal{C}^n = \mathbf{C}\mathcal{F}^* = \mathcal{C}, \quad \mathcal{C}_R^n = \mathbf{C}_R\mathcal{F}^*, \quad (55c)$$

so that the closed-loop system (54) becomes

$$\begin{bmatrix} \dot{z}^n(t) \\ \dot{\hat{z}}(t) \end{bmatrix} = \begin{bmatrix} A_{-1}^n + B^n\mathcal{C}_R^n + B_Q^n\mathcal{C}^n & B^n\mathcal{K} - B^n\mathcal{C}_R \\ \mathcal{P}\mathcal{C}^n + B_Q\mathcal{C}^n & A_{-1} - \mathcal{P}\mathcal{C} + \mathbf{B}\mathcal{K} \end{bmatrix} \begin{bmatrix} z^n(t) \\ \hat{z}(t) \end{bmatrix}. \quad (56)$$

We note that because  $\mathcal{F}$  is an isometry, the magnitude of the state of (54) equals that of (56), and thus, the stability properties follow from one another.

For the stability analysis, we introduce a virtual continuum state  $z$  with dynamics (6), (7) that serves as a continuum approximation of the  $n + m$  state  $\mathbf{z}$  (see [1, Thm 4]). That is, the parameters of the continuum system are connected to the  $n + m$  parameters according to (E.5), the input is the same as that of the  $n + m$  system, and the initial condition is taken as  $z_0 = \mathcal{F}\mathbf{z}_0$ . As the control input (10) is a well-posed output of the well-posed system (54), the input is locally  $L^2$ , and hence, the virtual continuum system has a well-posed solution  $z \in C([0, +\infty); E_c)$  for all  $z_0 \in E_c$ . However, in order to retain the continuum approximation accuracy, we, in fact, reset the virtual continuum state at  $t = kT$ , for  $k \in \mathbb{N}$  and some given  $T > 0$ , as  $z_{kT} = \mathcal{F}\mathbf{z}(kT) \in E_c$ , which, actually, results in  $z \in C([(k-1)T, kT]; E_c)$  for all  $k \in \mathbb{N}$ .

Let us denote by  $\tilde{z} = \hat{z} - z$  the virtual continuum estimation error. Now, writing  $z^n = z - (z - z^n)$ , we get the following virtual error dynamics based on (56) and using  $\mathcal{C}^n = \mathcal{C}$

$$\dot{\tilde{z}}(t) = (A_{-1} + \mathbf{B}\mathcal{C}_R + \mathcal{P}\mathcal{C})\tilde{z}(t) + (B_Q + \mathcal{P})\mathcal{C}(z(t) - z^n(t)), \quad (57)$$

which consists of internally exponentially stable dynamics plus a perturbation term depending on the continuum approximation error  $z - z^n$ . Using the virtual estimation error, the virtual continuum dynamics under the control law (10) can be written as

$$\dot{z}(t) = (A_{-1} + B_Q\mathcal{C} + \mathbf{B}\mathcal{K})z(t) + (\mathbf{B}\mathcal{K} - \mathbf{B}\mathcal{C}_R)\tilde{z}(t), \quad (58)$$

which consists of internally exponentially stable dynamics plus a perturbation term depending on the virtual estimation error. For the actual  $n + m$  system, the continuum observer-based control law contains additional error terms due to the kernel and parameter approximation. We write the term  $\mathcal{C}_R\hat{z}$  as

$$\begin{aligned} \mathcal{C}_R\hat{z}(t) &= \mathcal{C}_R^n\hat{z}(t) + (\mathcal{C}_R - \mathcal{C}_R^n)\hat{z}(t) \\ &= \mathcal{C}_R^n z^n(t) + \mathcal{C}_R^n(z(t) - z^n(t)) + \mathcal{C}_R^n\tilde{z}(t) \\ &\quad + (\mathcal{C}_R - \mathcal{C}_R^n)\hat{z}(t), \end{aligned} \quad (59)$$

<sup>5</sup>Note that we have  $B^n = B$  and  $\mathcal{C}^n = \mathcal{C}$ , as those operators only act on the  $\mathbf{v}$ -part of the state, which is unaffected by the transforms  $\mathcal{F}$  and  $\mathcal{F}^*$ .

which consists of the exact state feedback, a continuum approximation error, a virtual estimation error, and parameter approximation error (operating on the observer state). Performing the same steps with the term  $\mathcal{K}\hat{z}(t)$  in the control law, and by using  $\hat{z} = \tilde{z} + z$ , we get dynamics

$$\begin{aligned} \dot{z}^n(t) &= (A_{-1}^n + B_Q^n \mathcal{C}^n + B^n \mathcal{K}^n) z^n(t) \\ &\quad + B^n (\mathcal{K}^n - \mathcal{C}_R^n) (z(t) - z^n(t)) \\ &\quad + B^n (\mathcal{K} - \mathcal{C}_R) \tilde{z}(t) + B^n (\Delta \mathcal{K}^n - \Delta \mathcal{C}_R^n) z(t), \end{aligned} \quad (60)$$

where we additionally denote  $\Delta \mathcal{K}^n = \mathcal{K} - \mathcal{K}^n$  and  $\Delta \mathcal{C}_R^n = \mathcal{C}_R - \mathcal{C}_R^n$ .<sup>6</sup>

**Step 2** (stability properties of the nominal closed-loop system): Combining (57), (58), (60), the closed-loop dynamics for  $z^e := (\tilde{z}, z, z^n)$  can be written as

$$\dot{z}^e(t) = A_s z^e(t) + \begin{bmatrix} (B_Q + P)\mathcal{C} \\ 0 \\ B^n (\mathcal{K}^n - \mathcal{C}_R^n) \end{bmatrix} (z(t) - z^n(t)), \quad (61)$$

where we denote

$$A_s = \begin{bmatrix} A_{-1} + B\mathcal{C}_R + P\mathcal{C} & 0 & 0 \\ B(\mathcal{K} - \mathcal{C}_R) & A_{-1} + B_Q\mathcal{C} + B\mathcal{K} & 0 \\ B^n(\mathcal{K} - \mathcal{C}_R) & B^n(\Delta \mathcal{K}^n - \Delta \mathcal{C}_R^n) & A_{-1}^n + B_Q^n \mathcal{C}^n + B^n \mathcal{K}^n \end{bmatrix}, \quad (62)$$

which is exponentially stable due to the exponential stability of the diagonal entries by Lemma 1, [1, Thm 1], and Footnote 6, respectively. The perturbation term in (61) can be estimated via the continuum approximation error, which, however, is also dependent on the closed-loop state. Hence, as there is no guarantee that the operator acting on the continuum approximation error is small in norm, the state-dependent perturbation may negatively affect the exponential closed-loop stability. However, we establish next that, in fact, when the continuum approximation error is sufficiently small (for sufficiently large  $n$ ) the perturbation term does not destroy exponential stability of the closed-loop system.

Using variation of parameters, the solution to (61) can be written as

$$z^e(t) = \mathbb{T}_t z_0^e + \int_0^t \mathbb{T}_{(t-s)} \begin{bmatrix} (B_Q + P)\mathcal{C} \\ 0 \\ B^n (\mathcal{K}^n - \mathcal{C}_R^n) \end{bmatrix} (z(s) - z^n(s)) ds, \quad (63)$$

where by  $\mathbb{T}_t$  we denote the semigroup generated by the lower-triangular operator in (62). We define a perturbation as

$$\mathbf{d}(t) = \begin{bmatrix} d_1(t) \\ d_2(t) \end{bmatrix} := \begin{bmatrix} \mathcal{C} \\ \mathcal{K}^n - \mathcal{C}_R^n \end{bmatrix} (z(t) - z^n(t)), \quad (64)$$

<sup>6</sup>Here  $\mathcal{K}^n$  denotes an approximate, continuum-based stabilizing control kernel for the  $n + m$  system. For example, it can be viewed as an approximation of the continuum control kernels, in particular, for step approximation we have  $\mathcal{K}^n = \mathcal{F}\mathcal{F}^*\mathcal{K}$ . Such approximate, continuum-based control kernels remain stabilizing for the  $n + m$  system as the difference from the exact control kernel  $\Delta \mathcal{K}^n$  becomes arbitrarily small when  $n$  is sufficiently large (see [1, Lem. 5], [1, Thm 3], [15, Thm 3.4]).

and write  $z^e(t) = \mathbb{T}_t z_0^e + \Phi_t \mathbf{d}$ , where the input-to-state map  $\Phi_t$ , defined by

$$\Phi_t \mathbf{d} := \int_0^t \mathbb{T}_{(t-s)} \begin{bmatrix} B_Q + P & 0 \\ 0 & 0 \\ 0 & B^n \end{bmatrix} \mathbf{d}(s) ds, \quad (65)$$

can be bounded independently of  $t$  due to the exponential stability of the semigroup  $\mathbb{T}_t$  [30, Prop. 4.4.5]. Moreover, as  $\mathbb{T}_t$  is exponentially stable, the first term in (63) decays exponentially to zero. Hence, for every  $t \geq 0$ , there exist some  $M, \omega, M_\Phi > 0$  such that

$$\|z^e(t)\|_{E_c^3} \leq M e^{-\omega t} \|z_0^e\|_{E_c^3} + M_\Phi \|\mathbf{d}\|_{L^2([0,t]; \mathbb{R}^{2m})}. \quad (66)$$

**Step 3** (estimation of perturbation due to continuum approximation): The remaining step is to estimate the perturbation (64) in terms of the continuum approximation error, where we employ Proposition 2 from Appendix D. Moreover, as the input  $\mathbf{U}(t) = (\mathcal{K} - \mathcal{C}_R)\hat{z}(t)$  is a well-posed output of the closed-loop system (56), there exists an operator  $\Psi_t^{\text{cl}}$  such that  $\mathbf{U} = \Psi_t^{\text{cl}} \begin{pmatrix} z_0^n \\ \tilde{z}_0 \end{pmatrix}$ . Moreover, by using

$$\left\| \begin{bmatrix} \hat{z}(t) \\ z^n(t) \end{bmatrix} \right\|_{E_c^2} = \left\| \begin{bmatrix} 1 & 1 & 0 \\ 0 & 0 & 1 \end{bmatrix} z^e(t) \right\|_{E_c^2} \leq 2 \|z^e(t)\|_{E_c^3}, \quad (67)$$

for any fixed  $T > 0$ , we have the estimate by Proposition 2

$$\|\mathbf{d}\|_{L^2([0,T]; \mathbb{R}^{2m})} \leq \delta_1 \|\mathbf{z}_0\|_E + 2\delta_2 M_{\Psi_T^{\text{cl}}} \|z_0^e\|_{E_c^3}, \quad (68)$$

where  $M_{\Psi_T^{\text{cl}}} = \|\Psi_T^{\text{cl}}\|_{\mathcal{L}(E_c^2, L^2([0,T]; \mathbb{R}^{2m}))}$ . Thus, inserting (68) to (66) and using  $\|\mathbf{z}_0\|_E = \|z_0^n\|_{E_c} \leq \|z_0^e\|_{E_c^3}$ , we have, for any fixed  $T > 0$ , for  $t \in [0, T)$  that

$$\|z^e(t)\| \leq M e^{-\omega t} \|z_0^e\|_{E_c^3} + M_\Phi \left( \delta_1 + 2\delta_2 M_{\Psi_T^{\text{cl}}} \right) \|z_0^e\|_{E_c^3}. \quad (69)$$

Moreover, in order to retain the accuracy of the continuum approximation, we reset the virtual continuum state at  $t = T$  to  $z(T) = z_T = z^n(T^-)$ .<sup>7</sup> By [1, Thm 4] (analogously to Proposition 2) and using  $2M_{\Psi_T^{\text{cl}}} \|z_0^e\|_{E_c^3}$  as an upper bound for the input on  $t \in [0, T)$ , there exist some  $\delta_3, \delta_4 > 0$  such that

$$\|z(T^-) - z^n(T^-)\|_{E_c} \leq \delta_3 \|\mathbf{z}_0\|_E + 2\delta_4 M_{\Psi_T^{\text{cl}}} \|z_0^e\|_{E_c^3}. \quad (70)$$

Thus, after the reset we have

$$\begin{aligned} \|z_T^e\|_{E_c^3} &\leq \|z^e(T^-)\|_{E_c^3} + \left\| \begin{pmatrix} z(T^-) - z^n(T^-) \\ z(T^-) - z^n(T^-) \\ 0 \end{pmatrix} \right\|_{E_c^3} \\ &\leq M e^{-\omega T} \|z_0^e\|_{E_c^3} + M_\Phi \left( \delta_1 + 2\delta_2 M_{\Psi_T^{\text{cl}}} \right) \|z_0^e\|_{E_c^3} \\ &\quad + 2(\delta_3 + 2\delta_4 M_{\Psi_T^{\text{cl}}}) \|z_0^e\|_{E_c^3} \\ &\leq \left( M e^{-\omega T} + (M_\Phi + 2)(1 + 2M_{\Psi_T^{\text{cl}}}) \delta \right) \|z_0^e\|_{E_c^3}, \end{aligned} \quad (71)$$

<sup>7</sup>Notation  $T^- = T - \varepsilon$ , where  $\varepsilon > 0$  is arbitrarily small, indicates the time instance before the reset. Note that  $z^n$  and  $\tilde{z}$  are, in fact, continuous in time, so that  $z^n(T^-) = z^n(T)$  and  $\tilde{z}(T^-) = \tilde{z}(T)$ , as the resets concern only the virtual continuum state  $z$ .

where we denote  $\delta = \max_{i=1,\dots,4} \{\delta_i\}^8$  and use  $\|\mathbf{z}_0\|_E \leq \|z_0^e\|_{E_c^3}$ .

**Step 4** (derivation of stability estimate): The estimates (69)–(71) apply analogously on any interval  $t \in [kT, (k+1)T)$ , for any  $k \in \mathbb{N}$ , provided that  $z_0^e$  is replaced with the initial condition  $z_{kT}^e$  for that particular time interval. Hence, for any  $t \in [kT, (k+1)T)$ , we have

$$\begin{aligned} \|z^e(t)\| &\leq M e^{-\omega(t-kT)} \|z_{kT}^e\|_{E_c^3} \\ &\quad + M_\Phi \left(1 + 2M_{\Psi_T^{\text{cl}}}\right) \delta \|z_{kT}^e\|_{E_c^3}, \end{aligned} \quad (72)$$

where we can estimate

$$\|z_{kT}^e\|_{E_c^3} \leq \left(M e^{-\omega T} + (M_\Phi + 2)(1 + 2M_{\Psi_T^{\text{cl}}})\delta\right)^k \|z_0^e\|_{E_c^3}. \quad (73)$$

Now, if we fix  $T$  and  $n$  sufficiently large such that  $M e^{-\omega T} + (M_\Phi + 2)(1 + 2M_{\Psi_T^{\text{cl}}})\delta < 1 =: c$ , combining (72), (73) gives, for all  $t \in [kT, (k+1)T]$  with  $k \in \mathbb{N}$ ,

$$\begin{aligned} \|z^e(t)\|_{E_c^3} &\leq c^k \left(M e^{-\omega(t-kT)} + (M_\Phi + 2)(1 + 2M_{\Psi_T^{\text{cl}}})\delta\right) \\ &\quad \times \|z_0^e\|_{E_c^3}. \end{aligned} \quad (74)$$

Moreover, using  $c^k \leq e^{\frac{\log(c)}{T}t}$  for all  $t \in [kT, (k+1)T]$ , we have, for all  $t \geq 0$ ,

$$\|z^e(t)\|_{E_c^3} \leq \left(M + (M_\Phi + 2)(1 + 2M_{\Psi_T^{\text{cl}}})\delta\right) e^{-\bar{c}t} \|z_0^e\|_{E_c^3}, \quad (75)$$

where  $\bar{c} := -\frac{\log(c)}{T} > 0$  since  $c < 1$ , and thus, the closed-loop system (61) is exponentially stable on  $E_c^3$ . Consequently, considering the initialization of the virtual continuum state to  $z(0) = \mathcal{F}\mathbf{z}_0$  and using (67) with  $\|z^n\|_{E_c} = \|\mathbf{z}\|_E$  together with  $\|z_0^e\|_{E_c} \leq 3 \left\| \begin{bmatrix} \mathbf{z}_0 \\ \hat{z}_0 \end{bmatrix} \right\|_{E \times E_c}$  (that follows from the definition of  $z^e$ ), we have that

$$\begin{aligned} \left\| \begin{bmatrix} \mathbf{z}(t) \\ \hat{z}(t) \end{bmatrix} \right\|_{E \times E_c} &\leq 6 \left(M + (M_\Phi + 2)(1 + 2M_{\Psi_T^{\text{cl}}})\delta\right) \\ &\quad \times e^{-\bar{c}t} \left\| \begin{bmatrix} \mathbf{z}_0 \\ \hat{z}_0 \end{bmatrix} \right\|_{E \times E_c}, \end{aligned} \quad (76)$$

which concludes the proof.  $\square$

<sup>8</sup>We note that, for any fixed  $T > 0$ ,  $\delta$  depends only on the continuum approximation error of the parameters of the  $n + m$  system.

## 5. Numerical Example and Simulation Results

Consider an  $n + 2$  system (43), (44) with the following parameters for  $i, \ell = 1, \dots, n$

$$\lambda_i(x) = 1, \quad \mu_1(x) = 2, \quad \mu_2(x) = 1, \quad (77a)$$

$$\sigma_{i,\ell}(x) = x^3(x+1) \left(\frac{i}{n} - \frac{1}{2}\right) \frac{\ell}{n} \left(\frac{\ell}{n} - 1\right), \quad (77b)$$

$$W_{i,1}(x) = 3 \left(\frac{i}{n} - \frac{1}{2}\right), \quad W_{i,2}(x) = 2 \left(\frac{i}{n} - \frac{1}{2}\right), \quad (77c)$$

$$\theta_{1,i}(x) = -\frac{3i}{n} \left(\frac{i}{n} - 1\right), \quad \theta_{2,i}(x) = -\frac{2i}{n} \left(\frac{i}{n} - 1\right), \quad (77d)$$

$$\psi_{l,j}(x) = 0, \quad l, j \in \{1, 2\}, \quad (77e)$$

$$Q_{i,1} = 8 \left(\frac{i}{n} - \frac{1}{2}\right), \quad Q_{i,2} = -8 \left(\frac{i}{n} - 2\right), \quad (77f)$$

$$R_{1,i} = \cos\left(2\pi \frac{i}{n}\right), \quad R_{2,i} = 2 \frac{i}{n} \left(\frac{i}{n} + 5\right). \quad (77g)$$

Based on numerical experiments, the  $n + 2$  system with parameters (77) is open-loop unstable. Due to the particular structure of the parameters, respective continuum parameters satisfying (E.5) can be constructed as

$$\lambda(x, y) = 1, \quad \mu_1(x) = 2, \quad \mu_2(x) = 1, \quad (78a)$$

$$\sigma(x, y, \eta) = x^3(x+1) \left(y - \frac{1}{2}\right) \eta(\eta - 1), \quad (78b)$$

$$W_1(x, y) = 3 \left(y - \frac{1}{2}\right), \quad W_2(x, y) = 2 \left(y - \frac{1}{2}\right), \quad (78c)$$

$$\theta_1(x, y) = -3y(y - 1), \quad \theta_2(x, y) = -2y(y - 1), \quad (78d)$$

$$\psi_{i,j}(x) = 0, \quad i, j \in \{1, 2\} \quad (78e)$$

$$Q_1(y) = 8 \left(y - \frac{1}{2}\right), \quad Q_2(y) = -8(y - 2), \quad (78f)$$

$$R_1(y) = \cos(2\pi y), \quad R_2(y) = 2y(y + 5). \quad (78g)$$

The observer kernel equations (14)–(16) have explicit solution

$$M_1^1(x, \xi, y) = \left(y - \frac{1}{2}\right), \quad (79a)$$

$$M_1^2(x, \xi, y) = e^{x - \frac{1}{2}\xi - 1} \left(y - \frac{1}{2}\right), \quad (79b)$$

$$M_2^2(x, \xi, y) = e^{x - \xi} \left(y - \frac{1}{2}\right), \quad (79c)$$

$$N_{1,1}^1(x, \xi) = 0, \quad N_{1,1}^2(x, \xi) = 0, \quad (79d)$$

$$N_{2,1}^1(x, \xi) = 0, \quad N_{2,1}^2(x, \xi) = e^{x - \frac{1}{2}\xi - 1}, \quad (79e)$$

$$N_{1,2}^2(x, \xi) = 0, \quad N_{2,2}^2(x, \xi) = e^{x - \xi}, \quad (79f)$$

where  $M_1^\star(\cdot, y)$ ,  $N_{1,1}^\star$ , and  $N_{2,1}^\star$  are defined on  $\mathcal{T}_1^1 = \{(x, \xi) \in \mathcal{T} : \xi \geq 2x - 1\}$  and  $\mathcal{T}_1^2 = \{(x, \xi) \in \mathcal{T} : \xi \leq 2x - 1\}$  for the respective superindex  $\star = 1, 2$ , while  $M_2^2(\cdot, y)$ ,  $N_{2,1}^2$  and  $N_{2,2}^2$  are defined on  $\mathcal{T}_2^2 = \mathcal{T}$ , for each  $y \in [0, 1]$ . Note the

discontinuity in  $N_{2,1}$  along  $\xi = 2x - 1$ . The control kernels  $\mathbf{K}, \mathbf{L}$  are the same as in [1, (75)].

For the simulations, we approximate the  $n + 2$  system (43), (44) and the  $n + 2$  observer (47)–(49) using finite-differences with 128 grid points in  $x$ . The continuum observer (11)–(13) we implement as an  $\hat{n} + 2$  system, where  $\hat{n}$  is a degree of freedom for the numerical implementation, in which we employ finite-difference approximations for implementing the observer. For illustrating Theorem 4, we emulate the continuum by taking  $\hat{n} = 60$  and consider  $n < \hat{n}$ . For initial conditions, every state component of the  $n + m$  system is initialized to  $u_0(x) = v_0(x) = \frac{1}{2} \sin(2\pi x)$  and the observer is initialized to zero.

### 5.1. Illustration of Theorem 3

The simulation results for the output estimation errors and obtained control inputs from (46)–(49) are shown in Figures 1 and 2 for  $n = 8, 9, 10, 11$ . Consistently with Theorem 3, the estimation errors and the controls tend to zero faster as  $n$  increases, as the approximation error to the exact kernels becomes smaller as  $n$  increases. Moreover, the closed-loop system is unstable for  $n < 7$ , which is also consistent with Theorem 3, as large approximation errors in the kernels may lead to instability.

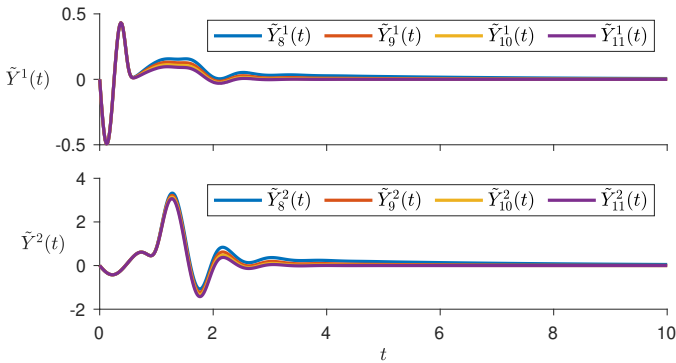


Figure 1: The output estimation errors of the observer (47)–(49) for  $\mathbf{Y}(t) = \mathbf{v}(0, t)$  from (43), (44) when  $n = 8, 9, 10, 11$ .

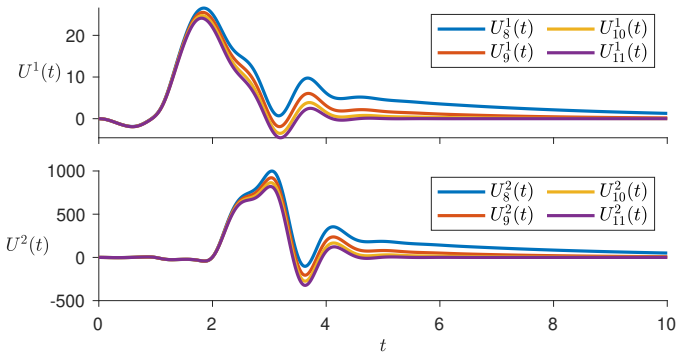


Figure 2: The controls  $\mathbf{U}(t)$  based on (46)–(48) in closed-loop with (43), (44) when  $n = 8, 9, 10, 11$ .

### 5.2. Illustration of Theorem 4

The simulation results for the output estimation errors and the obtained control inputs from (10)–(13), where the continuum is emulated by an  $\hat{n} + 2$  system with  $\hat{n} = 60$ , are shown in Figures 3 and 4 for  $n = 53, 55, 57, 59$  in (43), (44). Consistently with Theorem 4, the estimation errors and controls tend to zero faster as  $n$  tends towards  $\hat{n}$ . Interestingly, the initial transient behavior of the output estimation errors and control inputs is virtually the same for all  $n$  considered, which may be attributed to the initialization of the observer to zero and the transport delays in the dynamics. Finally, we note that, in this case, the closed-loop system is unstable for  $n < 50$ , which is also consistent with Theorem 4, as small  $n$  may destroy closed-loop stability.

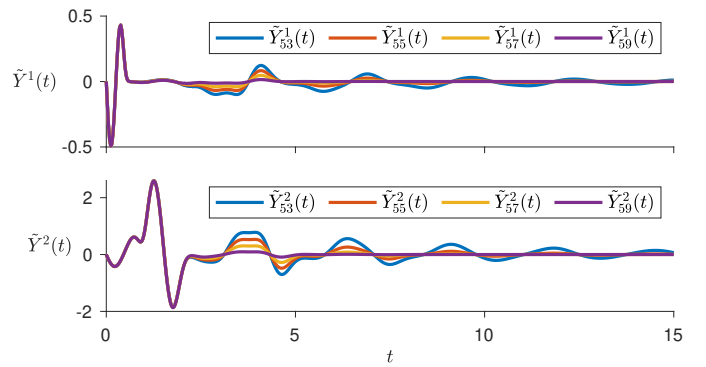


Figure 3: The output estimation errors of the continuum observer (11)–(13) for  $\mathbf{Y}(t) = \mathbf{v}(0, t)$  from (43), (44) when  $n = 53, 55, 57, 59$ .

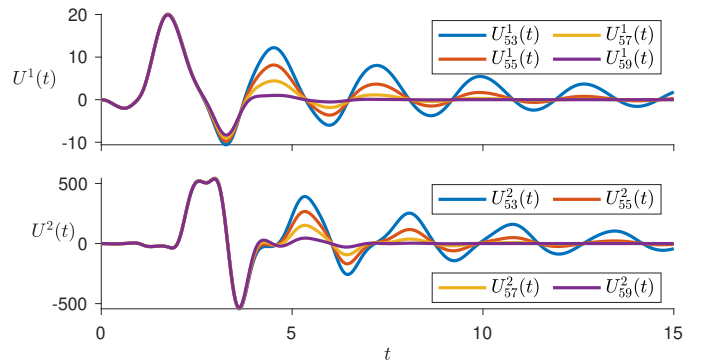


Figure 4: The controls  $\mathbf{U}(t)$  based on (10)–(12) in closed loop with (43), (44) when  $n = 53, 55, 57, 59$ .

We note that one could also consider the continuum observer implemented as an  $\hat{n} + m$  system with  $\hat{n} < n$ , as closed-loop stability is, in fact, retained under any approximate observer for which the approximation error related to the solutions is sufficiently small, such that  $c < 1$  holds in (74). In particular, implementation of the continuum observer as an  $\hat{n} + m$  system with  $\hat{n} < n$  illustrates a potential gain in computational complexity akin to a reduced-order observer. Such a benefit would be more evident as  $n$  increases, which would allow a continuum observer implementation of order  $\hat{n}$  (potentially much smaller than

$n$ ) to provide sufficiently accurate estimates of the  $n + m$  system's state, without being dominated by errors due to numerical approximation of the respective PDEs. Moreover, the accuracy of the continuum approximation depends on the choice of the particular numerical scheme employed for solving the continuum-based observer. For example, with spectral-based methods (see, e.g., [31]) one may obtain results in which the computational complexity benefits are more evident, even for smaller  $n$ . Although numerical computation of the continuum observer requires further investigation, the flexibility on the choice of numerical scheme and of the observer order  $\hat{n}$  may be practically significant, and they are enabled by our continuum-based approach for computing control/observer kernels and observer dynamics.

## 6. Conclusions and Future Work

We developed non-located, observer-based output-feedback law for a class of  $(\infty + m)$  continua of hyperbolic PDE systems. Moreover we employed the developed observer (and the respective observer kernels) in designing continuum observer-based output-feedback laws for the respective class of large-scale  $n + m$  hyperbolic PDEs. The motivation of such continuum-based control and observer designs is the potential gain in computational complexity/flexibility, as the computation of the continuum-based designs is independent of  $n$ . Utilization of the full potential of the proposed continuum-based designs calls for development of numerical methods to efficiently solve the continuum kernel equations (14)–(16), (E.2)–(E.4) and the observer dynamics (11)–(13). For the former, the power series method [12, 32] could constitute a promising approach, and for the latter, we anticipate spectral-based methods (see, e.g., [31]) to be potentially effective. Both of these are topics of our ongoing research.

## Appendix A. Derivation of the Observer Kernels

Let us first differentiate (29) with respect to  $x$  and use the Leibniz rule to get

$$\begin{aligned} \tilde{u}_x(t, x, y) &= \tilde{\alpha}_x(t, x) + \mathbf{M}(x, x, y)\tilde{\beta}(t, x) \\ &+ \int_0^x \mathbf{M}_x(x, \xi, y)\tilde{\beta}(t, \xi)d\xi, \end{aligned} \quad (\text{A.1})$$

$$\begin{aligned} \tilde{\mathbf{v}}_x(t, x) &= \tilde{\beta}_x(t, x) + \mathbf{N}(x, x)\tilde{\beta}(t, x) \\ &+ \int_0^x \mathbf{N}_x(x, \xi)\tilde{\beta}(t, \xi)d\xi. \end{aligned} \quad (\text{A.2})$$

Moreover, differentiating  $\tilde{u}$  in (29) with respect to  $t$  and using (26) gives

$$\begin{aligned} \tilde{u}_t(t, x) &= -\lambda(x, y)\tilde{\alpha}_x(t, x, y) + \int_0^1 \sigma(x, y, \eta)\tilde{\alpha}(t, x, \eta)d\eta \\ &+ \int_0^x \int_0^1 D_+(x, \xi, y, \eta)\tilde{\alpha}(t, \xi, \eta)d\eta d\xi \\ &+ \int_0^x \mathbf{M}(x, \xi, y)\mathbf{\Lambda}_-(\xi)\tilde{\beta}_\xi(t, \xi)d\xi \\ &+ \int_0^1 \int_0^x \mathbf{M}(x, \xi, y)\mathbf{\Theta}(\xi, \eta)\tilde{\alpha}(t, \xi, \eta)d\xi d\eta \\ &+ \int_0^x \int_0^1 \int_0^\xi \mathbf{M}(x, \xi, y)\mathbf{D}_-(x, s, \eta)\tilde{\alpha}(t, s, \eta)dsd\eta d\xi, \end{aligned} \quad (\text{A.3})$$

where integration by parts further gives

$$\begin{aligned} &\int_0^x \mathbf{M}(x, \xi, y)\mathbf{\Lambda}_-(\xi)\tilde{\beta}_\xi(t, \xi)d\xi = \\ &\mathbf{M}(x, x, y)\mathbf{\Lambda}_-(x)\tilde{\beta}(t, x) - \mathbf{M}(x, 0, y)\mathbf{\Lambda}_-(0)\tilde{\beta}(t, 0) \\ &- \int_0^x (\mathbf{M}_\xi(x, \xi, y)\mathbf{\Lambda}_-(\xi) + \mathbf{M}(x, \xi, y)\mathbf{\Lambda}'_-(\xi))\tilde{\beta}(t, \xi)d\xi. \end{aligned} \quad (\text{A.4})$$

Similarly, differentiating  $\tilde{\mathbf{v}}$  in (29) with respect to  $t$  and using (26) gives

$$\begin{aligned} \tilde{\mathbf{v}}_t(t, x) &= \mathbf{\Lambda}_-(x)\tilde{\beta}_x(t, x) + \int_0^1 \mathbf{\Theta}(x, y)\tilde{\alpha}(t, x, y)dy \\ &+ \int_0^x \int_0^1 \mathbf{D}_-(x, \xi, y)\tilde{\alpha}(t, \xi, y)dy d\xi \\ &+ \int_0^x \mathbf{N}(x, \xi)\mathbf{\Lambda}_-(\xi)\tilde{\beta}_\xi(t, \xi)d\xi \\ &+ \int_0^x \int_0^1 \mathbf{N}(x, \xi)\mathbf{\Theta}(\xi, y)\tilde{\alpha}(t, \xi, y)dy d\xi \\ &+ \int_0^x \int_0^1 \int_0^\xi \mathbf{N}(x, \xi)\mathbf{D}_-(x, s, y)\tilde{\alpha}(t, s, y)dsdy d\xi, \end{aligned} \quad (\text{A.5})$$

where integration by parts further gives

$$\begin{aligned} & \int_0^x \mathbf{N}(x, \xi) \mathbf{\Lambda}_-(\xi) \tilde{\boldsymbol{\beta}}_\xi(t, \xi) d\xi = \\ & \mathbf{N}(x, x) \mathbf{\Lambda}_-(x) \tilde{\boldsymbol{\beta}}(t, x) - \mathbf{N}(x, 0) \mathbf{\Lambda}_-(0) \tilde{\boldsymbol{\beta}}(t, 0) \\ & - \int_0^x (\mathbf{N}_\xi(x, \xi) \mathbf{\Lambda}_-(\xi) + \mathbf{N}(x, \xi) \mathbf{\Lambda}'_-(\xi)) \tilde{\boldsymbol{\beta}}(t, \xi) d\xi. \quad (\text{A.6}) \end{aligned}$$

Thus, in order for (24) to hold,  $\mathbf{M}, \mathbf{N}$  need to satisfy (14) with boundary conditions (15a), (15b), along with  $\mathbf{P}_+, \mathbf{P}_-$  satisfying (13), and  $D_+, \mathbf{D}_-$  satisfying (28). Moreover, evaluating (29) along  $x = 1$  and using the boundary conditions (25), (27) gives (15c) and (31).

## Appendix B. Well-posedness of (6), (7), (10)–(12)

**Proposition 1.** *The closed-loop system (6), (7), (10)–(12) is well-posed on  $E_c \times E_c$ .*

*Proof.* In order to write the closed-loop system (6), (7), (10)–(12) more compactly as an abstract Cauchy problem, define  $z(t) = (u(t, \cdot, \cdot), \mathbf{v}(t, \cdot))$ , and

$$Az(t) = \begin{bmatrix} -\lambda \partial_x & 0 \\ 0 & \mathbf{\Lambda}_- \partial_x \end{bmatrix} z(t) + Sz(t), \quad (\text{B.1})$$

where  $Sz(t)$  corresponds to the right-hand side of (6) and the domain of  $A$  is defined as

$$\begin{aligned} \mathcal{D}(A) &= \{z \in H^1([0, 1]; L^2([0, 1]; \mathbb{R}) \times \mathbb{R}^m) : \\ & u(0) = 0, \mathbf{v}(1) = 0\}. \quad (\text{B.2}) \end{aligned}$$

Moreover, denote by  $A_{-1}$  the (unique) extension of  $A$  from  $E_c$  to the dual space of  $\mathcal{D}(A)$  with respect to  $E_c$ , which exists by [30, Prop. 2.10.2] due to  $\mathcal{D}(A)$  being dense in  $E_c$ . In order to express the boundary couplings, define control operators  $B, B_Q$  according to the boundary traces in (7) as [30, Rem. 10.1.6]

$$B = \begin{bmatrix} 0 \\ \delta_1 \mathbf{\Lambda}_- \end{bmatrix}, \quad B_Q = \begin{bmatrix} \delta_0 \lambda \mathbf{Q} \\ 0 \end{bmatrix}, \quad (\text{B.3a})$$

where  $\delta_\star$  denotes the Dirac delta function at  $x = \star$ , and output operators  $\mathcal{C}, \mathcal{C}_R$  as

$$\mathcal{C}z(t) = \mathbf{v}(0, t), \quad \mathcal{C}_R z(t) = \int_0^1 \mathbf{R}(y) u(t, 1, y) dy. \quad (\text{B.4})$$

Moreover, define  $P, \mathcal{K}$  corresponding to the backstepping observer and controller gains as

$$P = \begin{bmatrix} \mathbf{P}_+ \\ \mathbf{P}_- \end{bmatrix}, \quad \mathcal{K}z(t) = \left\langle \begin{bmatrix} \mathbf{K}(1, \cdot, \cdot) \\ \mathbf{L}(1, \cdot) \end{bmatrix}, \begin{bmatrix} u(t) \\ \mathbf{v}(t) \end{bmatrix} \right\rangle_{E_c}, \quad (\text{B.5})$$

so that the closed-loop system (6), (7), (10)–(12) can be written as an abstract Cauchy problem

$$\begin{aligned} \begin{bmatrix} \dot{z}(t) \\ \dot{\hat{z}}(t) \end{bmatrix} &= \begin{bmatrix} A_{-1} + BC_R + B_Q \mathcal{C} & -BC_R + BK \\ PC + B_Q \mathcal{C} & A_{-1} - PC + BK \end{bmatrix} \begin{bmatrix} z(t) \\ \hat{z}(t) \end{bmatrix} \\ &= \left( \begin{bmatrix} A_{-1} & 0 \\ 0 & A_{-1} \end{bmatrix} + \begin{bmatrix} B & B & B_Q & 0 \\ B & 0 & B_Q & -P \end{bmatrix} \begin{bmatrix} 0 & \mathcal{K} \\ \mathcal{C}_R & -\mathcal{C}_R \\ \mathcal{C} & 0 \\ -\mathcal{C} & \mathcal{C} \end{bmatrix} \right) \begin{bmatrix} z(t) \\ \hat{z}(t) \end{bmatrix} \\ &=: (A_{-1}^e + B^e \mathcal{C}^e) \begin{bmatrix} z(t) \\ \hat{z}(t) \end{bmatrix}. \quad (\text{B.6}) \end{aligned}$$

Thus, (B.6) can be written in an output feedback form, and by [33, Thm 13.1.12] the closed-loop system is well-posed if the inverse of  $I - \mathbf{G}^e(s)$  exists and is bounded for all  $\text{Re}(s)$  sufficiently large, where  $\mathbf{G}^e$  is the transfer function of the triple  $(A^e, B^e, \mathcal{C}^e)$ . By virtue of [33, Lem. 13.1.14], the well-posedness of the closed-loop system is independent of the (bounded) in-domain coupling terms  $Sz(t), S\hat{z}(t)$ , meaning that it suffices to consider the transfer function  $\mathbf{G}^e$ , which can be computed by [34, Thm 2.9] from

$$su(s, x, y) = -\lambda(x, y) u_x(s, x, y), \quad (\text{B.7a})$$

$$s\mathbf{v}(s, x) = \mathbf{\Lambda}_-(x) \mathbf{v}_x(s, x), \quad (\text{B.7b})$$

$$s\hat{u}(s, x, y) = -\lambda(x, y) \hat{u}_x(s, x, y) - \mathbf{P}_+(x, y) \mathbf{U}_4(s), \quad (\text{B.7c})$$

$$s\hat{\mathbf{v}}(s, x) = \mathbf{\Lambda}_-(x) \hat{\mathbf{v}}_x(s, x) - \mathbf{P}_-(x) \mathbf{U}_4(s), \quad (\text{B.7d})$$

$$\mathbf{v}(s, 1) = \mathbf{U}_1(s) + \mathbf{U}_2(s), \quad (\text{B.7e})$$

$$\hat{\mathbf{v}}(s, 1) = \mathbf{U}_1(s), \quad (\text{B.7f})$$

$$u(s, 0, y) = \mathbf{Q}(y) \mathbf{U}_3(s), \quad (\text{B.7g})$$

$$\hat{u}(s, 0, y) = \mathbf{Q}(y) \mathbf{U}_3(s), \quad (\text{B.7h})$$

$$\begin{aligned} \mathbf{Y}_1(s) &= \int_0^1 \int_0^1 \mathbf{K}(1, \xi, y) \hat{u}(s, \xi, y) dy d\xi \\ &+ \int_0^1 \mathbf{L}(1, \xi) \hat{\mathbf{v}}(s, \xi) d\xi, \quad (\text{B.7i}) \end{aligned}$$

$$\mathbf{Y}_2(s) = \int_0^1 \mathbf{R}(y) (u(s, 1, y) - \hat{u}(s, 1, y)) dy, \quad (\text{B.7j})$$

$$\mathbf{Y}_3(s) = \mathbf{v}(s, 0), \quad \mathbf{Y}_4(s) = \hat{\mathbf{v}}(s, 0) - \mathbf{v}(s, 0), \quad (\text{B.7k})$$

where  $(\mathbf{Y}_i(s))_{i=1}^4 = \bar{\mathbf{G}}^e(s) (\mathbf{U}_i(s))_{i=1}^4$ . Since  $P$  and  $\mathcal{K}$  are bounded operators, the components of  $\bar{\mathbf{G}}^e$  involving them necessarily tend to zero as  $\text{Re}(s) \rightarrow \infty$ . The remaining components can be computed based on the general solution

$$u(s, x, y) = a(y) \exp\left(-s \int_0^x \lambda(\zeta, y) d\zeta\right), \quad (\text{B.8a})$$

$$\mathbf{v}(s, x) = \exp\left(s \int_0^x \mathbf{\Lambda}_-(\zeta) d\zeta\right) \mathbf{b}, \quad (\text{B.8b})$$

to (B.7a), (B.7b) (respectively for  $\hat{u}$ ,  $\hat{v}$ ), where the coefficients  $a$ ,  $\mathbf{b}$  are solved for from the boundary conditions of (B.7). We obtain (for  $\mathbf{U}_4 \equiv 0$ )

$$\begin{bmatrix} \mathbf{Y}_2(s) \\ \mathbf{Y}_3(s) \\ \mathbf{Y}_4(s) \end{bmatrix} = \begin{bmatrix} 0 & 0 & 0 \\ \exp\left(-s \int_0^1 \boldsymbol{\Lambda}_-(x) dx\right) & \exp\left(-s \int_0^1 \boldsymbol{\Lambda}_-(x) dx\right) & 0 \\ 0 & -\exp\left(-s \int_0^1 \boldsymbol{\Lambda}_-(x) dx\right) & 0 \end{bmatrix} \begin{bmatrix} \mathbf{U}_1(s) \\ \mathbf{U}_2(s) \\ \mathbf{U}_3(s) \end{bmatrix}, \quad (\text{B.9})$$

which concludes that  $\text{Re } \bar{\mathbf{G}}_e(s) \rightarrow 0$  as  $\text{Re}(s) \rightarrow \infty$  due to the diagonal matrix  $\boldsymbol{\Lambda}_-$  satisfying  $\boldsymbol{\Lambda}_- > 0$  by Assumption 1. Thus, the inverse of  $I - \bar{\mathbf{G}}^e(s)$  exists and is bounded when  $\text{Re}(s)$  is sufficiently large, and hence, the closed-loop system is well-posed by [33, Thm 13.1.12, Lem. 13.1.14]. That is, for all  $z_0, \hat{z}_0 \in E_c$ , there exists a unique solution  $z, \hat{z} \in C([0, \infty); E_c)$  to (B.6).  $\square$

### Appendix C. Well-posedness of (54)

The operator in (54) splits into a feedback form

$$\begin{bmatrix} \mathbf{A}_{-1} + \mathbf{B}\mathbf{C}_R + \mathbf{B}_Q\mathbf{C} & \mathbf{B}\mathbf{K} - \mathbf{B}\mathbf{C}_R \\ \mathbf{P}\mathbf{C} + \mathbf{B}_Q\mathbf{C} & \mathbf{A}_{-1} - \mathbf{P}\mathbf{C} + \mathbf{B}\mathbf{K} \end{bmatrix} = \begin{bmatrix} \mathbf{A}_{-1} & 0 \\ 0 & \mathbf{A}_{-1} \end{bmatrix} + \begin{bmatrix} \mathbf{B} & \mathbf{B} & \mathbf{B}_Q & 0 \\ \mathbf{B} & 0 & \mathbf{B}_Q & -\mathbf{P} \end{bmatrix} \begin{bmatrix} 0 & \mathcal{K} \\ \mathbf{C}_R & -\mathcal{C}_R \\ \mathbf{C} & 0 \\ -\mathbf{C} & \mathcal{C} \end{bmatrix}, \quad (\text{C.1})$$

so that the well-posedness of the closed-loop system (54) can be studied similarly to Appendix B. The changes required to Appendix B are, in fact, relatively minor and merely involve replacing  $u$  with  $\mathbf{u}$  and the respective continuum operators with the  $n + m$  counterparts. For example, (B.7a) becomes  $s\mathbf{u}(s, x) = -\boldsymbol{\Lambda}_+(x)\mathbf{u}_x(s, x)$ . By repeating the computations of Appendix B, we get a transfer function that is almost identical to the one shown in (B.9) (ignoring  $\mathbf{Y}_1$  and  $\mathbf{U}_4$  due to  $\mathbf{P}$  and  $\mathcal{K}$  being bounded operators), with the exception of the transfer function from  $\mathbf{U}_3$  to  $\mathbf{Y}_2$  being

$$\begin{aligned} \frac{\mathbf{Y}_2(s)}{\mathbf{U}_3(s)} &= \frac{1}{n} \mathbf{R} \exp\left(-s \int_0^1 \boldsymbol{\Lambda}_+(\zeta) d\zeta\right) \mathbf{Q} \\ &\quad - \int_0^1 \mathbf{R}(y) \exp\left(-s \int_0^1 \lambda(\zeta, y) d\zeta\right) \mathbf{Q}(y) dy, \end{aligned} \quad (\text{C.2})$$

where the real part of both terms tends to zero as  $\text{Re}(s) \rightarrow \infty$  due to  $\lambda > 0$ ,  $\boldsymbol{\Lambda}_+ > 0$  by Assumptions 1 and 2. Hence, the closed-loop system (54) is well-posed by the same arguments as those at the end of Appendix B.

### Appendix D. Continuum Approximation Result for Well-Posed Outputs

In [1, Thm 4] we have shown that the solution of an  $\infty + m$  system (6), (7) can approximate the solution of a

respective  $n + m$  system (43), (44) to arbitrary accuracy on compact time intervals, provided that the parameters, initial conditions, and inputs of the two systems are appropriately connected to one another. In Proposition 2, we state the respective result for outputs.

**Proposition 2.** *Consider an  $n + m$  system (43), (44) with parameters  $\mu_j, \psi_{j,\ell}, \theta_{j,i}, w_{i,j}, q_{i,j}, \lambda_i$ , and  $\sigma_{i,l}$  for  $i, l = 1, \dots, n$  and  $j, \ell = 1, \dots, m$ , satisfying Assumption 2, initial conditions  $(\mathbf{u}_0, \mathbf{v}_0) \in E$ , and a control input  $\mathbf{U} \in L^2_{\text{loc}}([0, +\infty); \mathbb{R}^m)$ . Construct a continuum system (6), (7) with parameters  $\lambda, \mu_j, \sigma, \theta_j, W_j, Q_j, \psi_{j,\ell}$  for  $j, \ell = 1, \dots, m$  that satisfy Assumption 1 and (E.5), and equip (6), (7) with initial conditions  $(u_0 = \mathcal{F}_n \mathbf{u}_0, \mathbf{v}_0)$  and the same input  $\mathbf{U}$ . Consider an output space  $\mathcal{Y}$  (a Hilbert space) and take an output  $\mathbf{Y}^n(t) = \mathcal{C}_a^n \begin{pmatrix} \mathbf{u}(t) \\ \mathbf{v}(t) \end{pmatrix}$  from the  $n + m$  system and the respective output  $\mathbf{Y}(t) = \mathcal{C}_a \begin{pmatrix} u(t) \\ \mathbf{v}(t) \end{pmatrix}$  from the  $\infty + m$  system, such that  $\mathbf{Y}^n, \mathbf{Y} \in L^2_{\text{loc}}([0, \infty), \mathcal{Y})$ , i.e., such that the outputs are well-posed. On any compact interval  $t \in [0, T]$ , for any given  $T > 0$ , we have*

$$\|\mathbf{Y} - \mathbf{Y}^n\|_{L^2([0, T]; \mathcal{Y})} \leq \delta_1 \|(\mathbf{u}_0, \mathbf{v}_0)\|_E + \delta_2 \|\mathbf{U}\|_{L^2([0, T]; \mathbb{R}^m)}, \quad (\text{D.1})$$

where  $\delta_1, \delta_2 > 0$  become arbitrarily small when  $n$  is sufficiently large.

*Proof.* The proof is analogous to the respective proof for the solutions [1, Thm 4] (see also [2, Thm 6.1]). Namely, considering any well-posed output  $\mathbf{Y}$  of the continuum system (6), (7), there exist families of bounded linear operators  $\Psi_t, \mathbb{F}_t$  for  $t \geq 0$ , depending continuously on the parameters of (6), (7), such that the output is given by

$$\mathbf{Y} = \Psi_t \begin{pmatrix} u_0 \\ \mathbf{v}_0 \end{pmatrix} + \mathbb{F}_t \mathbf{U}. \quad (\text{D.2})$$

Now, considering the respective output  $\mathbf{Y}^n$  of the  $n + m$  system (43), (44) and transforming the system into  $E_c$  through  $\mathcal{F}$ , we get the respective form of the output of the  $n + m$  system as

$$\mathbf{Y}^n = \Psi_t^n \begin{pmatrix} \mathcal{F}_n u_0 \\ \mathbf{v}_0 \end{pmatrix} + \mathbb{F}_t^n \mathbf{U}. \quad (\text{D.3})$$

Subtracting (D.3) from (D.2) and denoting  $\delta_1 = \|\Psi_T - \Psi_T^n\|_{\mathcal{L}(E_c, L^2([0, T]; \mathcal{Y}))}$ ,  $\delta_2 = \|\mathbb{F}_T - \mathbb{F}_T^n\|_{\mathcal{L}(L^2([0, T]; \mathbb{R}^m), L^2([0, T]; \mathcal{Y}))}$ , the claim follows after using  $u_0 = \mathcal{F}_n \mathbf{u}_0$  and recalling that  $\mathcal{F}_n$  is an isometry. In particular,  $\delta_1, \delta_2$  become arbitrarily small when  $n$  is sufficiently large due to (E.5) and the continuous dependence of the output on the parameters.  $\square$

### Appendix E. Backstepping-Based State-Feedback Stabilization of (6), (7) and its Application to Stabilization of (43), (44)

If the full state information of the system (6), (7) is available, we have shown in [1, Thm 1] that the system

can be exponentially stabilized by the state-feedback law

$$\begin{aligned} \mathbf{U}(t) = & \int_0^1 \int_0^1 \mathbf{K}(1, \xi, y) u(t, \xi, y) dy d\xi \\ & + \int_0^1 \mathbf{L}(1, \xi) \mathbf{v}(t, \xi) d\xi - \int_0^1 \mathbf{R}(y) u(t, 1, y) dy, \end{aligned} \quad (\text{E.1})$$

which is of the same form as (10) but with the estimated states replaced by the actual states. The control kernels  $\mathbf{K} \in L^\infty(\mathcal{T}; L^2([0, 1]; \mathbb{R}^m))$ ,  $\mathbf{L} \in L^\infty(\mathcal{T}; \mathbb{R}^{m \times m})$  satisfy the control kernel equations

$$\begin{aligned} \mathbf{\Lambda}_-(x) \mathbf{K}_x(x, \xi, y) - \mathbf{K}_\xi(x, \xi, y) \lambda(\xi, y) - \mathbf{K}(x, \xi, y) \lambda_\xi(\xi, y) = \\ \mathbf{L}(x, \xi) \mathbf{\Theta}(\xi, y) + \int_0^1 \mathbf{K}(x, \xi, \eta) \sigma(\xi, \eta, y) d\eta, \end{aligned} \quad (\text{E.2a})$$

$$\begin{aligned} \mathbf{\Lambda}_-(x) \mathbf{L}_x(x, \xi) + \mathbf{L}_\xi(x, \xi) \mathbf{\Lambda}_-(\xi) + \mathbf{L}(x, \xi) \mathbf{\Lambda}'_-(\xi) = \\ \mathbf{L}(x, \xi) \mathbf{\Psi}(\xi) + \int_0^1 \mathbf{K}(x, \xi, y) \mathbf{W}(\xi, y) dy, \end{aligned} \quad (\text{E.2b})$$

with boundary conditions

$$-\mathbf{\Theta}(x, y) = \mathbf{K}(x, x, y) \lambda(x, y) + \mathbf{\Lambda}_-(x) \mathbf{K}(x, x, y), \quad (\text{E.3a})$$

$$\mathbf{\Psi}(x) = \mathbf{L}(x, x) \mathbf{\Lambda}_-(x) - \mathbf{\Lambda}_-(x) \mathbf{L}(x, x), \quad (\text{E.3b})$$

$$L_{i,j}(x, 0) = \frac{1}{\mu_j(0)} \int_0^1 K_i(x, 0, y) \lambda(0, y) Q_j(y) dy, \quad \forall i \leq j, \quad (\text{E.3c})$$

$$L_{i,j}(1, \xi) = l_{i,j}(\xi), \quad \forall j < i, \quad (\text{E.3d})$$

where  $l_{i,j}$  are arbitrary due to (E.3d) being an artificial boundary condition to guarantee well-posedness of the control kernel equations. We choose  $l_{i,j}$  such that

$$l_{i,j}(1) = -\frac{\psi_{i,j}(1)}{\mu_i(1) - \mu_j(1)}, \quad (\text{E.4})$$

in order to make the artificial boundary condition compatible with (E.3b) at  $(1, 1)$ . Note that the boundary conditions for  $\mathbf{L}(0, 0)$  are, in general, overdetermined due to (E.3b) and (E.3c), (E.3a), which stems potential discontinuities in the  $\mathbf{L}$  kernels.

Moreover, we have shown in [1, Sect. 4–5] that (6), (7) can be viewed as a continuum approximation of (43), (44) by connecting the parameters of (6), (7) to the parameters of (43), (44) such that  $\theta_j, W_j, Q_j, R_j, \lambda$ , and  $\sigma$

are continuous functions satisfying Assumption 1 with

$$\theta_j(x, i/n) = \theta_{j,i}(x), \quad (\text{E.5a})$$

$$W_j(x, i/n) = w_{i,j}(x), \quad (\text{E.5b})$$

$$Q_j(i/n) = q_{i,j}, \quad (\text{E.5c})$$

$$R_j(i/n) = r_{j,i}, \quad (\text{E.5d})$$

$$\lambda(x, i/n) = \lambda_i(x), \quad (\text{E.5e})$$

$$\sigma(x, i/n, l/n) = \sigma_{i,l}(x), \quad (\text{E.5f})$$

for all  $x \in [0, 1]$ ,  $i, l = 1, \dots, n$  and  $j = 1, \dots, m$ .<sup>9</sup> In particular, by [1, Thm 3], the state-feedback control law

$$\mathbf{U}(t) = \frac{1}{n} \int_0^1 \tilde{\mathbf{K}}(1, \xi) \mathbf{u}(t, \xi) d\xi + \int_0^1 \tilde{\mathbf{L}}(1, \xi) \mathbf{v}(t, \xi) d\xi - \frac{1}{n} \mathbf{R} \mathbf{u}(t, 1), \quad (\text{E.6})$$

exponentially stabilizes the  $n + m$  system (43), (44) on  $E$ , where the control gains  $\tilde{\mathbf{K}}, \tilde{\mathbf{L}}$  are taken based on the continuum control kernels  $\mathbf{K}, \mathbf{L}$  in (E.2)–(E.4) as

$$\tilde{\mathbf{K}}(x, \xi) = \mathcal{F}_n^* \mathbf{K}(x, \xi, \cdot), \quad \tilde{\mathbf{L}}(x, \xi) = \mathbf{L}(x, \xi), \quad (\text{E.7})$$

where  $\mathcal{F}_n^*$  is given in (4).

## References

- [1] J.-P. Humaloja, N. Bekiaris-Liberis, Backstepping control of continua of linear hyperbolic PDEs and application to stabilization of large-scale  $n + m$  coupled hyperbolic PDE systems, arXiv, 2410.22067 (2024).
- [2] J.-P. Humaloja, N. Bekiaris-Liberis, Stabilization of a class of large-scale systems of linear hyperbolic PDEs via continuum approximation of exact backstepping kernels, IEEE Trans. Automat. Control (2025) 1–16.
- [3] V. Bikia, Non-invasive monitoring of key hemodynamical and cardiac parameters using physics-based modelling and artificial intelligence, Ph.D. thesis, EPFL (2021).
- [4] P. Reymond, F. Merenda, F. Perren, D. Rufenacht, N. Stergiopoulos, Validation of a one-dimensional model of the systemic arterial tree, Am. J. Physiol. Heart Circ. Physiol. 297 (2009) H208–H222.
- [5] L. Zhang, H. Luan, Y. Lu, C. Prieur, Boundary feedback stabilization of freeway traffic networks: ISS control and experiments, IEEE Trans. Control Syst. Technol. 30 (2022) 997–1008.
- [6] M. Herty, A. Klar, Modeling, simulation, and optimization of traffic flow networks, SIAM J. Sci. Comput. 25 (2003) 1066–1087.
- [7] H. Yu, M. Krstic, Output feedback control of two-lane traffic congestion, Automatica 125 (2021) Paper No. 109379.
- [8] G. Bastin, J.-M. Coron, Stability and Boundary Sabilization of 1-D Hyperbolic Systems, Birkhäuser/Springer, [Cham], 2016.
- [9] A. Diagne, M. Diagne, S. Tang, M. Krstic, Backstepping stabilization of the linearized *saint-venant-exner* model, Automatica 76 (2017) 345–354.
- [10] L. Guan, C. Prieur, L. Zhang, C. Prieur, D. Georges, P. Bellemain, Transport effect of COVID-19 pandemic in France, Annu. Rev. Control 50 (2020) 394–408.

<sup>9</sup>As noted in [2, Sect. IV.A], there are infinitely many ways to construct continuous (or even smooth in  $y$ ) functions satisfying (E.5) and Assumption 1 based on parameters satisfying Assumption 2.



- [11] C. Kitsos, G. Besancon, C. Prieur, High-gain observer design for a class of quasi-linear integro-differential hyperbolic systems-application to an epidemic model, *IEEE Trans. Automat. Control* 67 (2022) 292–303.
- [12] J.-P. Humaloja, N. Bekiaris-Liberis, On computation of approximate solutions to large-scale backstepping kernel equations via continuum approximation, *Syst. Control Lett.* 196 (2025) 105982.
- [13] V. Alleaume, M. Krstic, Ensembles of hyperbolic PDEs: Stabilization by backstepping, *IEEE Trans. Automat. Control* 70 (2025) 905–920.
- [14] F. Di Meglio, R. Vazquez, M. Krstic, Stabilization of a system of  $n + 1$  coupled first-order hyperbolic linear PDEs with a single boundary input, *IEEE Trans. Automat. Control* 58 (2013) 3097–3111.
- [15] L. Hu, F. Di Meglio, R. Vazquez, M. Krstic, Control of homodirectional and general heterodirectional linear coupled hyperbolic PDEs, *IEEE Trans. Automat. Control* 61 (2016) 3301–3314.
- [16] J. Auriol, F. Bribiesca Argomedo, Output-feedback stabilization of  $n + m$  linear hyperbolic ODE-PDE-ODE systems, *IFAC-PapersOnLine* 58 (2024) 202–207.
- [17] J. Auriol, Output-feedback stabilization of an underactuated network of  $N$  interconnected  $n + m$  hyperbolic PDE systems, *IEEE Trans. Automat. Control* (2024) 1–12.
- [18] T. Enderes, J. Gabriel, J. Deutscher, Cooperative output regulation for networks of hyperbolic systems using adaptive cooperative observers, *Automatica* 162 (2024) 111506.
- [19] J. Auriol, D. Bresch-Pietri, Robust state-feedback stabilization of an underactuated network of interconnected  $n + m$  hyperbolic PDE systems, *Automatica* 136 (2022) 110040.
- [20] J. Auriol, F. Di Meglio, Minimum time control of heterodirectional linear coupled hyperbolic PDEs, *Automatica* 71 (2016) 300–307.
- [21] J.-M. Coron, L. Hu, G. Olive, Finite-time boundary stabilization of general linear hyperbolic balance laws via Fredholm backstepping transformation, *Automatica* 84 (2017) 95–100.
- [22] F. Di Meglio, F. Bribiesca Argomedo, L. Hu, M. Krstic, Stabilization of coupled linear heterodirectional hyperbolic PDE-ODE systems, *Automatica* 87 (2018) 281–289.
- [23] L. Hu, R. Vazquez, F. Di Meglio, M. Krstic, Boundary exponential stabilization of 1-dimensional inhomogeneous quasi-linear hyperbolic systems, *SIAM J. Control Optim.* 57 (2) (2019) 963–998.
- [24] L. Bhan, Y. Shi, M. Krstic, Neural operators for bypassing gain and control computations in PDE backstepping, *IEEE Trans. Automat. Control* (2024).
- [25] S.-S. Wang, M. Diagne, M. Krstic, Backstepping neural operators for  $2 \times 2$  hyperbolic PDEs, *arXiv*, 2312.16762v3 (2024).
- [26] J. Qi, J. Zhang, M. Krstic, Neural operators for PDE backstepping control of first-order hyperbolic PIDE with recycle and delay, *Syst. Control Lett.* 185 (2024) 105714.
- [27] J. Auriol, K. A. Morris, F. Di Meglio, Late-lumping backstepping control of partial differential equations, *Automatica* 100 (2019) 247–259.
- [28] H. Hochstadt, *Integral Equations*, Wiley Classics Edition, John Wiley & Sons, 1989.
- [29] K.-J. Engel, R. Nagel, *One-Parameter Semigroups for Linear Evolution Equations*, Springer, 2000.
- [30] M. Tucsnak, G. Weiss, *Observation and Control for Operator Semigroups*, Birkhäuser Verlag AG, 2009.
- [31] D. Kopriva, *Implementing Spectral Methods for Partial Differential Equations*, Springer Science & Business Media, 2009.
- [32] R. Vazquez, G. Chen, J. Qiao, M. Krstic, The power series method to compute backstepping kernel gains: theory and practice, in: *IEEE Conf. Decis. Control*, 2023, pp. 8162–8169.
- [33] B. Jacob, H. Zwart, *Linear Port-Hamiltonian Systems on Infinite-dimensional Spaces*, Birkhäuser, 2012.
- [34] A. Cheng, K. A. Morris, Well-posedness of boundary control systems, *SIAM J. Control Optim.* 42 (4) (2003) 1244–1265.